EGG-WM-9502

Idaho National Engineering Laboratory

Managed by the U.S. Department of Energy

EGG-WM-9502
DECEMBER 1990

INFORMAL REPORT

HYDROLOGIC MODELING STUDY OF POTENTIAL FLOODING AT THE SUBSURFACE DISPOSAL AREA FROM A HYPOTHETICAL BREACH OF DIKE 2 AT THE IDAHO NATIONAL ENGINEERING LABORATORY

RICHARD C. MARTINEAU
DANIEL H. HOGGAN
KAREN N. KECK
THOMAS R. WOOD

~~2-23-95~~
L. Duguay 12-6 00

EG&G Idaho

Work performed under DOE Contract No. DE-AC07-76ID01570

EGG-WM-9502
DECEMBER 1990

INFORMAL REPORT

HYDROLOGIC MODELING STUDY OF POTENTIAL FLOODING AT THE SUBSURFACE DISPOSAL AREA FROM A HYPOTHETICAL BREACH OF DIKE 2 AT THE IDAHO NATIONAL ENGINEERING LABORATORY

RICHARD C. MARTINEAU
DANIEL H. HOGGAN
KAREN N. KECK
THOMAS R. WOOD

EGG-WM-9502

HYDROLOGIC MODELING STUDY OF POTENTIAL FLOODING AT THE SUBSURFACE DISPOSAL AREA FROM A HYPOTHETICAL BREACH OF DIKE 2 AT THE IDAHO NATIONAL ENGINEERING LABORATORY

Richard C. Martineau
Daniel H. Hoggan
Karen N. Keck
Thomas R. Wood

Published December, 1990

Idaho National Engineering Laboratory
EG&G Idaho, Inc.
Idaho Falls, Idaho 83415

Prepared for the
U.S. Department of Energy
Idaho Operations Office
Under DOE Contract NO. DE-AC07-76IDO1570

ABSTRACT

The Radioactive Waste Management Complex is located in the southwestern portion of the Idaho National Engineering Laboratory and stores solid radioactive wastes generated in national defense and research programs in two main disposal and storage areas: The Transuranic Storage Area (TSA) and the Subsurface Disposal Area (SDA). The SDA is surrounded by a series of perimeter berms designed to protect the SDA from local flooding due to heavy precipitation and rapid snow melt. This report uses two models to determine if the current SDA berm is sufficient to prevent floodwater from entering the SDA assuming the worst case scenario of the hypothetical Mackay Dam failure coupled with the 1965 Big Lost River Flood.

This investigation shows that the SDA berm is in danger of being overtopped by a breach flood under the most extreme case investigated. The extreme case is defined as a Dike 2 breach 62 ft wide at the top and 31 ft wide at the bottom. In this case, the water-level elevation of 5014.36 ft above msl would overtop the SDA berm at the southwest access-road crossing and for a distance of 500 ft next to the constriction near the southeast corner. At this water surface level, there would also be a small outflow around the west end of the SDA. This flow would cross over the saddle in the west access road and into the low areas on the north side. There is a possibility of a small amount of flow overtopping the SDA berm at the west access-road crossing if this should occur.

EXECUTIVE SUMMARY

The Radioactive Waste Management Complex (RWMC) is located in the southwestern portion of the Idaho National Engineering Laboratory (INEL) and approximately 1 mile east of the Diversion Area. RWMC encompasses 144 acres and consists of two main disposal and storage areas: the Transuranic Storage Area (TSA) and the Subsurface Disposal Area (SDA). Solid radioactive wastes generated in national defense and research programs is stored at the RWMC. The SDA is surrounded by a series of perimeter berms designed to protect the SDA from local flooding due to heavy precipitation and rapid snowmelt. The objective of this report is to determine if the current SDA berm is sufficient to prevent floodwater, from Spreading Area B in the event Dike 2 failed, from entering the SDA.

Two models were employed to analyze the flood routing near SDA. The first was designed to determine the potential volume of water for varying water surface elevations in INEL Diversion Area and is referred to as the INEL Diversion Area Flow System Model. This model will be used to simulate a worst case scenario to determine the maximum possible water level that could be held behind Dike 2. The worst case scenario used in this study is the hypothetical Mackay Dam failure coupled with the 1965 Big Lost River flood. This scenario represents the practical limit of water able to discharge in the Big Lost River. The second model will use the maximum water surface elevation in Spreading Area B and model several different types of Dike 2 breaches. The flood route from the breach and the flood levels will be determined to see if what, if any, danger the SDA berm is in.

The model simulation time of the INEL Diversion Area during a hypothetical Mackay is 50 days (1200 hours) and coincides with the 1965 flood hydrograph. A Mackay Dam failure is considered to be the practical limit of water available to discharge in the Big Lost River Drainage Basin. To simulate maximum inflow into Spreading Area A, the peak flow at the INEL Diversion Dam due to a Mackay Dam failure must coincide with the peak flow recorded in the 1965 flood. For the model, the failure of the dam occurs at 480 hours into the simulation.

The model predicts that at 508 hours into the simulation, the water surface elevation in Spreading Area A reaches a maximum of 5055.92 ft above msl. The water surface elevation in spreading areas B, C, and D is 5037.31 ft above msl, which is the elevation that water just begins to flow through the Dike 3 Weir into the Offsite Spreading Area. At this point in time, Area A contains approximately 23,600 acre-ft of water and areas B, C, and D contain a total of 16,500 acre-ft of water.

Previous calculations (Bennett, 1986) predict that when the Diversion Channel is running at peak discharge (7200 ft^3/s), Dike 1 near the Diversion Dam begins to be overtopped when the water surface elevation in Spreading Area A reaches an elevation of 5054.8 ft above msl. This is due to the backwater effect in the Diversion Channel. With a maximum predicted water surface elevation of 5055.92 ft above msl, not only will the Diversion Dam fail but a large portion of Dike 1 forming the Diversion Channel will

probably erode away. The model does not take into account the possible failure of a portion of Dike 1. If a portion of Dike 1 fails, the peak water surface elevations in the spreading areas will probably be less.

At 577 hours into the simulation, the peak water surface elevation of 5043.02 ft above msl is reached in Spreading Areas B, C, D and the Offsite Spreading Area. This water surface elevation is still 9.98 ft below the top of Dike 2 (5053 ft above msl) but is 2.4 ft over the top of Dike 3 (5040.6 ft above msl). The combined storage of areas B, C, and D is approximately 25,400 acre-ft of water. The Offsite Spreading Area will contain approximately 5,840 acre-ft of water at 5043.02 ft above msl. At this point in time, the water surface elevation of Area A is 5049.25 ft above msl. Area A will contain approximately 5730 acre-ft of water. The total storage in the Diversion Area will be approximately 37,000 acre-ft of water.

Breach parameters, selected to bracket the range of breach conditions reported in the literature, excluding the two that were considered non applicable, were applied to the flood routing and water surface profile models developed for this investigation and are shown in Table I-1.

Table I-1 Breach parameters

	Low	High
Maximum WS elevation behind dike (ft)	5043.0	5043.0
Breach bottom elevation (ft)	5034.7	5034.7
Breach bottom width (ft)	17	31
Breach side slopes	1:1	1:1
Breach-failure time (hr)	1	1

A sensitivity analysis of failure times from 0.1 to 4 hours indicated that within the range of values suggested in the literature, this parameter has insignificant effect on the peak discharge produced by the breach. Another comparative analysis of side slopes (H:V) from 0.1 to 2 revealed that this parameter can make a substantial difference in the peak discharge. A slope of 1:1 was selected because it fits the conditions of the rock fill at Dike 2. These two sets of conditions defined by the low and high criteria produced the following peak discharges at the breach: low = 1733 ft^3/s and high = 2759 ft^3/s.

Results in routing the breach hydrograph downstream with the model incorporating the Muskingum-Cunge (M-C) channel routing method compared almost identically with the results of the model using modified-Puls (M-P) channel routing. The peak discharges produced by the two models for the other flows at key locations appear in Table I-2.

Table I-2 Peak discharges at key locations

Location		Peak Discharges (ft^3/s) M-C	M-P
Flow over the railroad embankment	Low	1712	1712
	High	2728	2728
Inflow to detention basin southeast side of SDA from split-flow reach	Low	411	414
	High	797	887
Inflow to detention basin southeast side of SDA from main-flow reach	Low	1301	1302
	High	1930	1932
Outflow from detention basin at constriction near the southeast corner of SDA	Low	1573	1573
	High	2115	2115
Lower end of study reach at east of security facility	Low	1573	1567
	High	2114	2111
Outflow around southwest corner of the SDA	Low	97	97
	High	507	507

Final water-surface elevations next to the SDA, computed with HEC-2 based on the final peak discharges computed in the lower reach, appear in Table I-3

Table I-3 Final water-surface elevations next to SDA

Location		Peak Discharge (ft^3/s)	W S Elevation (ft)
Constriction near southeast corner of SDA (detention basin outlet - cross section 24)	Low	1567	5011.29
	High	2111	5013.84
Constriction between SDA and TSA about 300 ft north of SDA southeast corner (cross section 19)	Low	1567	5011.29
	High	2111	5011.89
Drainage channel about 400 ft southeast of security facility (cross section 4)	Low	1567	5007.78
	High	2111	5008.14

This investigation has shown that the SDA berm is in danger of being overtopped by a breach flood under the most extreme case investigated. The extreme case is defined as a Dike 2 breach 62 ft wide at the top and 31 ft wide at the bottom. In this case, the water-level elevation of 5014.36 ft above msl would overtop the SDA berm at the southwest access-road crossing and for a distance of 500 ft next to the constriction near the southeast corner. At this water surface level, there would also be a small outflow around the west end of the SDA. This flow would cross over the saddle in the west access road and into the low areas on the north side. There is a possibility of a very small amount of flow overtopping the SDA berm at the west access-road crossing if this should occur.

Along the northeast berm next to the TSA, especially near the southeast corner, the water surface elevations are close to or slightly above the top. There also would be some flow through the TSA on the east side of the barrel storage pad and on the east side of the covered storage facility.

The existing drainage channel east of the SDA is not sufficient to carry floods generated under either "low" or "high" breach criteria without overtopping of its banks. Under either set of parameters, the flow would be out of the banks, and there would be several inches of water over the pavement near the security facility and other buildings along Adams Boulevard.

Since there would be a very large volume of water stored behind Dike 2 at the maximum water level elevation of 5043.0 ft, there would be considerable exposure of the breach to erosive action of the outflow. According to the criteria developed by MacDonald and Langridge-Monopolis (1984) this would result in a very wide breach in a very short time. Of course, this would result in a very high peak discharge that would cause considerable

flooding at the SDA. However, if a wide breach were to be eroded by the large volume of water flowing through the breach, it seems more likely due to the composition of the riprap embankment (very large rocks) that the development of the breach would take place over a relatively long duration of time. In which case, the peak discharge would be relatively small.

CONTENTS

FIGURES

TABLES

ACRONYMS

PMF	probable maximum flood
RWMC	Radioactive Waste Management Complex
SDA	Subsurface Disposal Area
TAN	Test Area North
TSA	Transuranic Storage Area
USGS	U. S. Geological Survey

1 INTRODUCTION

The Radioactive Waste Management Complex (RWMC) is located in the southwestern portion of the Idaho National Engineering Laboratory (INEL) and approximately 1 mile east of the INEL Diversion Area (see Figure 1-2). The RWMC encompasses 144 acres and consists of two main disposal and storage areas: The Transuranic Storage Area (TSA) and the Subsurface Disposal Area (SDA). Solid radioactive waste generated in national defense and research programs is stored at the RWMC.

The SDA consists of below ground pits and trenches and one above ground storage pad. Both radioactive intermediate and low-level solid and liquid, TRU and mixed fission product, and nonradioactive hazardous wastes were disposed of in the trenches. TRU waste typically include cloth, paper, plastics, metals, rubber, and concrete contaminated with TRU radionuclides. Liquid organic waste was solidified in calcium silicate and vacuum packed in polybags within 55-gallon drums.

The SDA is surrounded by a series of perimeter berms designed to protect the SDA from local flooding because of heavy precipitation and rapid snow melt. The objective of this report is to determine if the current SDA berm is sufficient to prevent floodwater from entering the SDA in the event Dike 2 failed.

Two models were employed to analyze the flood routing near SDA. The first was designed to determine the potential volume of water for varying water surface elevations in the Diversion Area and is referred to as the INEL Diversion Area Flow System Model. This model was used to simulate a worst case scenario to determine the maximum possible water level that could be held behind Dike 2. The worst case scenario used in this study is the hypothetical Mackay Dam failure coupled with the 1965 Big Lost River flood. This scenario represents the practical limit of water able to discharge in the Big Lost River. The second model used the maximum water surface elevation in Spreading Area B and model several different types of Dike 2 breaches. The flood route from the breach and the flood levels were determined to see if what, if any, danger the SDA berm is in.

1.1 Big Lost River Drainage Basin

The Big Lost River Valley is one of the major structural intermountain basins of east-central Idaho. This valley encompasses an area of 1,410 mi^2 in Butte and Custer counties on the northwest side of the of the Eastern Snake River Plain, as shown in Figure 1-1.

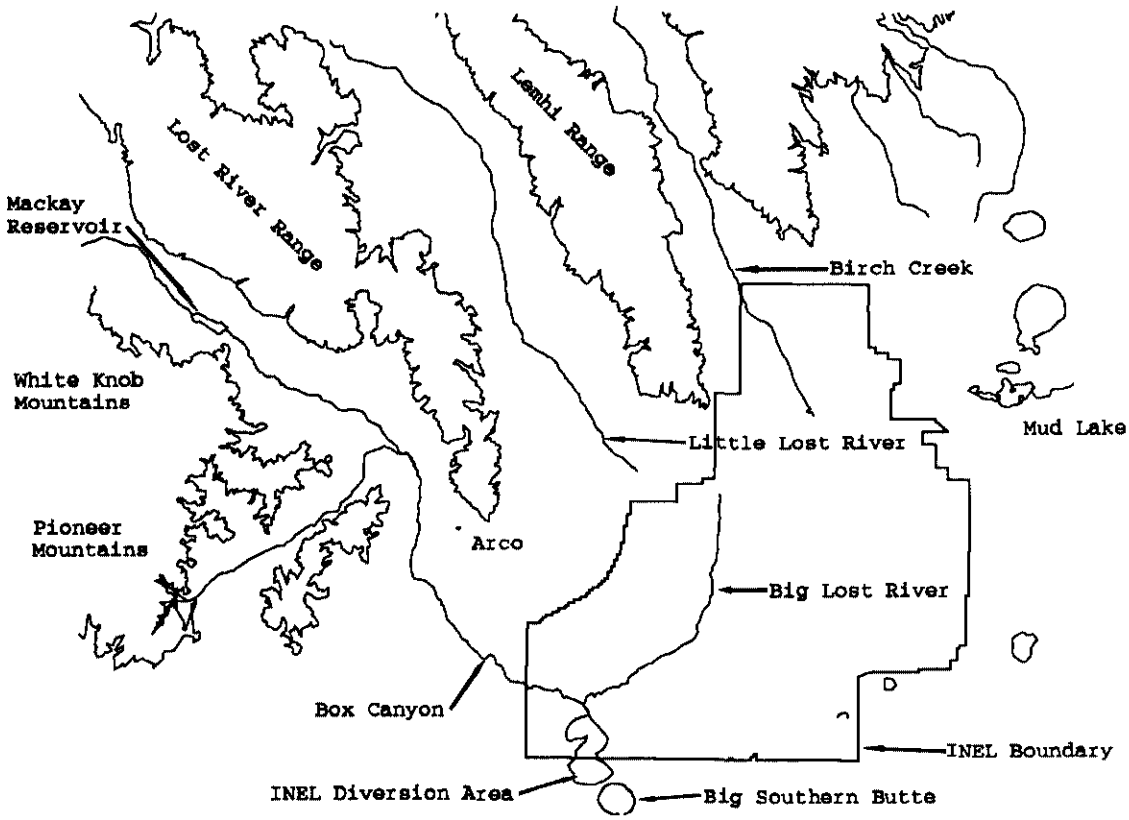

Figure 1-1 The Big Lost River drainage

Streamflow in the Big Lost River originates in the Lost River, Boulder, Pioneer, and White Knob mountain ranges.

The main stem of the Big Lost River is formed by the confluence of its East Fork and North Fork about 22 mi northwest of Mackay Dam, which impounds the river flows approximately 4 mi northwest of Mackay. The drainage basin above the dam has an area of 788 mi^2. A significant portion of the natural streamflow is controlled by the dam, which stores runoff for irrigation.

The Big Lost River flows southeast from the dam down the Big Lost River Valley past Arco onto the Snake River Plain. Southeast of Arco, the river enters Box Canyon, a narrow canyon approximately 5 mi long, with an average height of 50 to 55 ft and a width of 130 ft. The walls of the canyon are composed of fractured basalt and are nearly vertical. The river exits Box Canyon and flows to the Diversion Area, as shown in Figure 1-2.

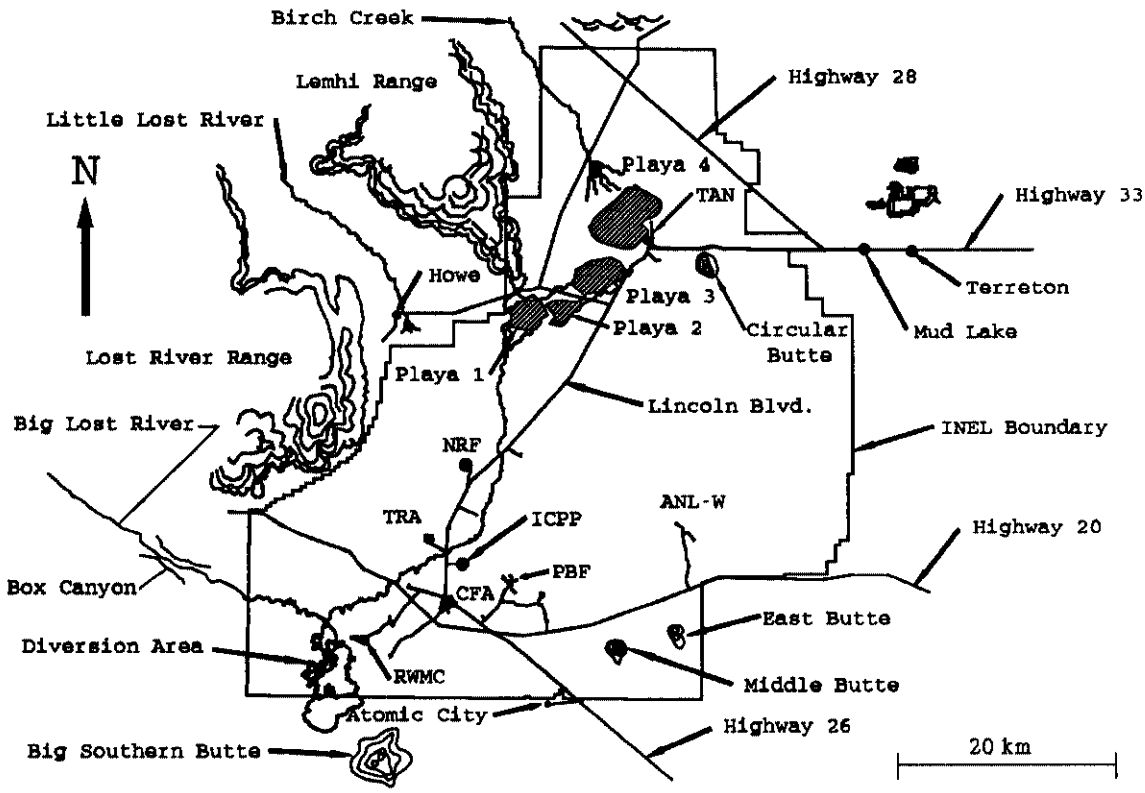

Figure 1-2 INEL topographic features showing the Big Lost River drainage basin

The Diversion Area was constructed in 1958 to divert high runoff flows from INEL facilities. The diversion system consists of a diversion dam, diversion channel, two 6-ft diameter gated culverts, three dikes, four spreading areas, one overflow spreading area located offsite, and two interconnecting channels (see Figure 1-3). The diversion channel is capable of carrying 7,200 ft^3/s of water from the Big Lost River into the spreading areas. Two low swales located southwest of the main channel will carry an additional 2,100 ft^3/s of water for a combined maximum diversion channel flow capacity of 9,300 ft^3/s (Bennett, 1986). The total capacity of the spreading areas is 18,200 acre-ft at 5,040 ft above Mean Sea Level (msl) and 58,000 acre-ft at an elevation of 5,050 ft above msl (McKinney, 1985).

Flows not diverted at the diversion dam, pass northward across the INEL in a shallow, gravel and silt channel. this main channel branches into several channels 18 mi northeast of the diversion dam, forming four shallow playas, referred to as the Big Lost River Sinks (see Figure 1-2).

The Big Lost River is in a topographically closed basin with no surface drainage to the Snake River. Instead, Big Lost River waters are lost to evaporation or infiltrate into the ground, recharging the Snake River Plain Aquifer. The basin is principally composed of coarse-grained materials with moderate-to-high infiltration rates. Infiltration and depression

storage losses are most significant at the Darlington Sinks, Big Lost River Sinks, and in Box Canyon, because of fractured basalt. Stream flows are often depleted before reaching the INEL by irrigation diversions and infiltration losses along the river. However, in times of heavy runoff, the river flows to its terminus in the Big Lost River Sinks at the northwest corner of the INEL.

1.1.1 Mackay Dam

Mackay Dam is approximately 4 mi northwest of Mackay, in Custer County, Idaho, Section 12, Township 7 North, Range 23 East, Boise Meridian. The dam impounds a 44,500 acre-ft reservoir on the Big Lost River. Construction of the dam began in 1905 and finished in 1917. It was built to provide irrigation water for 33,000 acres of agricultural lands in the Big Lost River Irrigation District and is now also used for recreational purposes.

Mackay Dam is classified as a high hazard dam by the State of Idaho (State of Idaho, 1978) with reference to the U.S. Army Corps of Engineers guidelines for safety inspection of dams (Corps of Engineers, 1977). This high hazard classification is based on the concentration of people and property downstream, the size of the dam, and the dam storage capacity it is not based on any aspect of the dam's current condition.

Since construction began, the possible consequences of a failure of the dam have been of concern to downstream residents. A seepage of 50 to 170 ft^3/s of water through the dam and the location of the dam near a fault that bounds the central area of the White Knob Mountains are the primary concerns (Nelson and Ross, 1969). Interest in a failure of Mackay Dam was heightened by the October 1983 Borah Peak earthquake, centered 11 mi northwest of the dam with a surface wave magnitude of 7.3, although the earthquake caused no structural damage to the dam.

1.1.2 INEL Diversion Area

The need for flood control on the INEL was first recognized in the early 1950s when the Test Reactor Area (TRA) and Idaho Chemical Processing Plant (ICPP) were threatened by localized flooding as a result of ice jams on the Big Lost River. The INEL Diversion Area was constructed in 1958 to divert high runoff flows from downstream INEL facilities, not for flood protection of the RWMC. The Diversion Area is located in the southwestern part of the INEL, about 4 mi east of the southwestern boundary (see Figure 1-2). The drainage area of the Big Lost River upstream from the diversion dam is about 1,450 mi^2 (Bennett, 1986). The diversion area is a cascade reservoir system consisting of a diversion dam, diversion channel, two 6-ft diameter gated culverts, three dikes, four spreading areas, one overflow spreading area located offsite, and two interconnecting channels as shown in Figure 1-3.

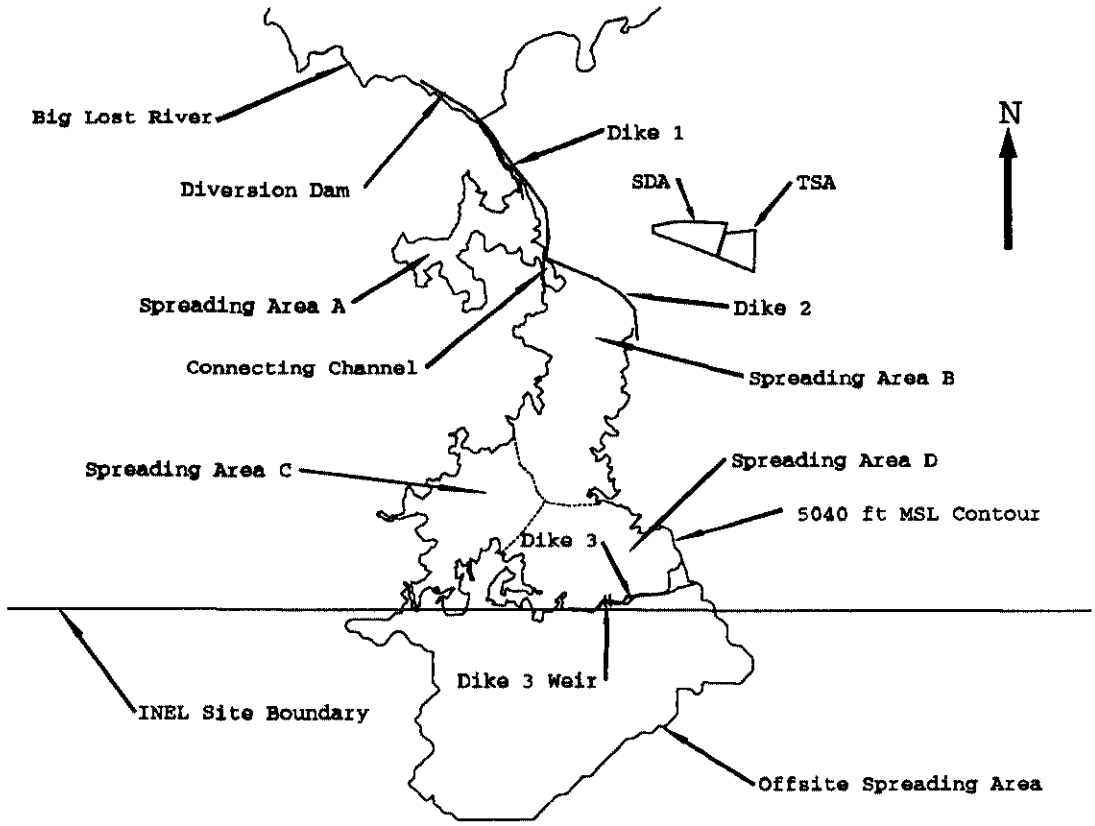

Figure 1-3 Diversion Area

The diversion channel was excavated through several basalt ridges and intervening surficial sedimentary deposits to connect the Big Lost River with a series of natural depressions. The depressions are designated as Spreading Areas A, B, C, and D. Big Lost River flows are diverted into the diversion channel by a low earthen dam across the Big Lost River. The dam is part of a long, continuous dike along the left side of the river and diversion channel. The configuration of the channel is unusually rough. Resistant basalt ridges create an irregular channel bottom that cause riffles and waterfalls at low to medium flows.

Two 6-ft diameter corrugated metal pipes permit passage of less than 900 ft^3/s through the dam into the river (Lamke, 1969). Flow in the river is regulated by gates on the culverts. During high flows, flow in excess of that allowed to pass through the culverts is carried by the Diversion Channel. Flow in the diversion channel is uncontrolled at discharges that exceed the capacity of the culverts. The diversion channel extends about 0.9 mi from the point of diversion to Spreading Area A. Water flows from Spreading Area A through the connecting channel into the three other spreading areas. An overflow weir at Dike 3 in Spreading Area D allows water to drain southwest to the Offsite Spreading Area, off the INEL boundary. Big Lost river flows have never been sufficient to exceed the capacity of the spreading areas and overflow the weir.

During 1965, a record snowpack was recorded in the Big Lost River drainage basin, resulting in record high streamflows in the Big Lost River. These streamflows were diverted to the INEL diversion system during the last nine months of that year. A peak discharge of 1,800 ft^3/s into the diversion channel occurred on June 29, 1965. From June 10, 1965, to the end of the year, 115,000 acre-ft of water flowed into the diversion dam. Area A contained 2,300 acre-ft of water, Area B contained 4,300 acre-ft of water, Area C contained 5,000 acre-ft of water, and Area D was dry (Barraclough et al., 1967). A measured infiltration rate of 0.7 ft/d in Area A was observed by the U. S. Geological Survey (USGS) (Barraclough et al., 1967). In Area B, the average infiltration rate was 2.6 ft/d. Several exposed basalt ridges in the floor of Area B resulted in high infiltration rates, whereas, in Area A, siltation has resulted in a lower infiltration rate.

High streamflows and a severe cold spell during the winter of 1983 to 1984 caused ice jams that imposed a danger of localized flooding. Ice buildup in Spreading Area A resulted in waters backing up in the diversion channel and ultimately threatening to overtop Dike 1. The high discharges to the spreading areas in 1983 and 1984 were largely the result of the Borah Peak earthquake of October 28, 1983. The earthquake created new springs upstream of Mackay Reservoir which increased the inflows to the reservoir significantly. In addition, outflows from the reservoir were increased to reduce the storage behind the dam. In response to this flood threat, upgrades to the Diversion Area were made to provide additional flood control, with a design criteria of increasing the diversion channel flow capacity of 2,500 ft^3/s to over 6,600 ft^3/s (McKinney, 1985).

The USGS performed a study to determine the new capacity of the diversion channel subsequent to enlarging the channel and raising the dike elevations (Bennett, 1986). The study concluded the diversion channel is capable of carrying 7,200 ft^3/s from the Big Lost River into the spreading areas. Two low swales located southwest of the main channel will carry and additional 2,100 ft^3/s for a combined maximum diversion capacity of 9,300 ft^3/s (Bennett, 1986). The total capacity of the spreading areas is 18,200 acre-ft at 5,040 ft above msl, and 58,000 acre-ft at 5,050 ft above msl (McKinney, 1985).

During winter months, nearly all flow is diverted to the spreading areas to avoid accumulation of ice in the main channel, reducing the possibility of flooding at downstream INEL facilities. Other periods of high discharge have resulted in much of the flow diverted to the spreading areas to prevent downstream flooding on the INEL. Significant annual discharges of water to the diversion channel occurred in the following years: 1969, diverting 108,050 acre-ft; 1983, diverting 206,450; and 1984 diverting 274,800 acre-ft. The high discharges to the spreading areas in 1969 were the result of high rates of snowmelt runoff in the basin. The high discharges to the spreading areas in 1983 and 1984 were largely the result of the Borah Peak earthquake. Flows in the Big Lost River were continuous at the diversion dam from April 1982 through December 1985. However, the dry weather from 1985 to 1989 resulted in little or no water being diverted to the spreading areas.

Spreading Area B is less than 1 mi west of the SDA. A failure of Dike 2 at

Spreading Area B could result in potential flooding at the RWMC. The RWMC, with an average elevation of 5,000 ft above msl is less than one mile northeast of Dike 2 at an elevation of 5,053 ft above msl at the top. The lower elevation and an access road on the west side of the SDA provides a direct route for floodwater should a failure of Dike 2 occur when there is sufficient water stored in Spreading Area B. The floodwater released from this hypothetical failure should require high velocities and flood stages to actually overtop or breach the existing peripheral dike and allow floodwater to enter the SDA. A failure of Dike 2 is unlikely, and the spreading grounds historically have contained low levels of water.

1.2 Dike 2 and SDA Vicinity

1.2.1 General Surface Drainage Conditions at SDA Site

The SDA, the TSA, and associated security and other support facilities form the RWMC; they are located together in an area of low relief relative to most of the surrounding topography. Except on the east side, the adjacent higher land surfaces extending out from this site a distance of a few hundred feet to a few thousand feet drain inward toward the site. Figure 1-4 illustrates the general topography in the RWMC area.

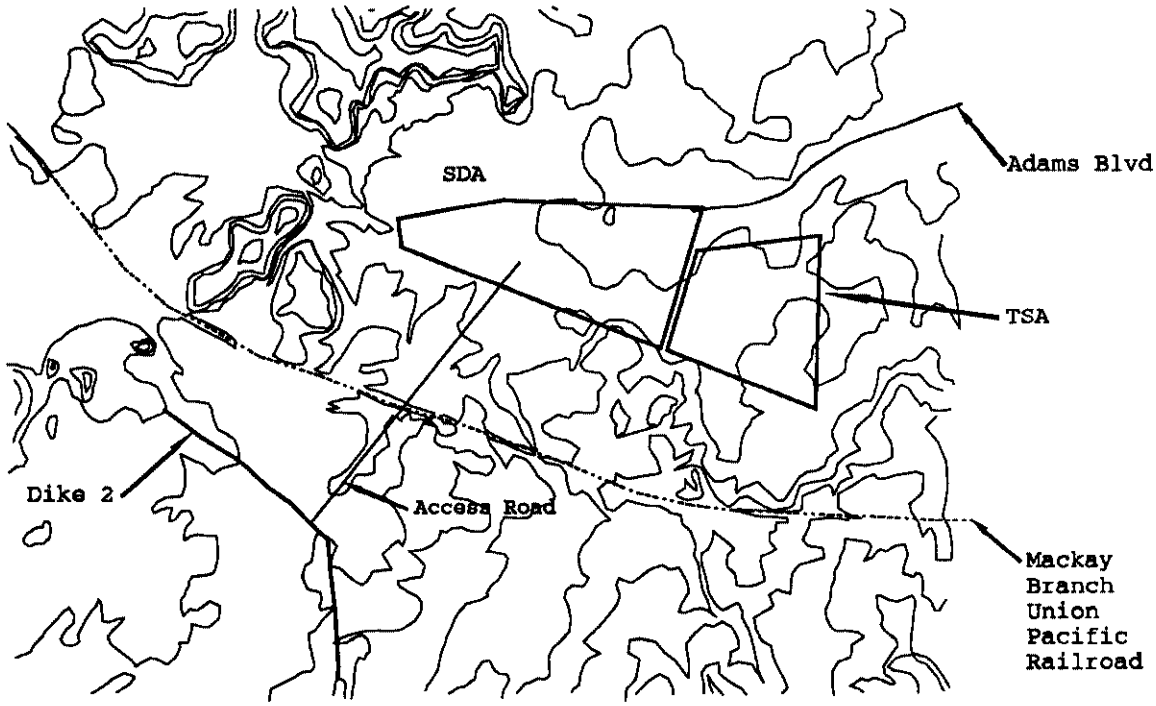

Figure 1-4 Topography of SDA-TSA Vicinity

Surface elevations range from 5006 to 5015 ft above msl at the SDA to as high as 5091 ft

above msl along one of the ridges on the adjacent watershed divide.

The topography of the SDA area slopes in an easterly direction (generally along the route of Adams Boulevard) in an area of lower relief and provides for drainage away from the site. An unlined drainage channel approximately 20-ft wide by 5 to 7-ft deep has been constructed in this area to dispose of runoff that accumulates next to the perimeter embankment of the SDA. This channel carries the excess water from proximity of the SDA into the low areas of the desert located to the east. Prior to the construction of this channel, there were instances of significant ponding of surface runoff next to the SDA.

1.2.2 The Potential Flood Threat of a Failure at Dike 2

The primary concern in this investigation is for the potential impact on the SDA of flood flows originating from a hypothetical failure of Dike 2 and the release of impounded water in Spreading Area B on the SDA. The large volume of water that could be impounded behind Dike 2 under extreme circumstances would be close to the SDA (3/4 mi) and several feet higher (35 ft).

Because the top of Dike 2 is at elevation 5053 ft above msl, and the maximum water level to be anticipated in Spreading Area B is 5043.02 ft above msl, overtopping of the dike as a source of flooding can be ruled out. The embankment would have to settle 10-ft for overtopping to occur. Thus, a breach in Dike 2 at the most critical location is the hypothetical failure that is most realistic to investigate. At its closest point, Dike 2 is about 3/4 mi southwest of the SDA perimeter embankment. This point on the dike is located approximately where the access road extending from the southwest side of the SDA crosses over Dike 2 (see Figure 1-4). A Dike 2 breach located on the west side of this road crossing would produce flood flows with maximum impact to the SDA. Natural depressions and valleys in the land surface between Dike 2 and the SDA would provide the shortest and most effective paths available for flood flows to reach the SDA. The elevation of the toe of the inside slope of Dike 2 fill also is lowest at this point (5034.7 ft above msl), providing conditions for the greatest depth of breach if the breach were to open up down to base of the embankment.

1.2.3 Nature of the Flood Threat to the SDA

Because a drainage system exists to carry excess runoff from the SDA to the desert areas of lower relief to the east, major inundation by ponding, as might be expected with an interior drainage basin, can be eliminated as a potential threat. Thus, the primary flood threat to the SDA from a breach in Dike 2 is from the peak discharge and associated high water levels that would be generated and not from the total volume of water that would be released.

Although the potential volume of water that could be in storage behind Dike 2 may seem overwhelming in comparison to the small amount of storage available in the depressions

in the vicinity of the site, the flood volume by itself is of less concern as a hazard in this situation than the peak discharge of the flood flow. The peak discharge that will determine the water surface elevations of the flood flow at various locations on the site. The height of these water surface elevations will determine whether the existing drainage system will contain the flood and where and to what extent the embankment at the SDA may be overtopped.

1.2.4 Characteristics of Dike 2

Dike 2 is massive at the critical location identified for investigating a potential breach. The embankment has a top width of 25 to 30 ft and relatively steep side slopes, approximately 1 to 1. It appears to be constructed of and clay, silt, and gravel construction. The faces of the dike are covered with basalt rock to act as riprap. The rocks vary in weight from a few pounds to several hundred pounds and are in evidence on both faces of the dike from bottom to top.

1.2.5 Characteristics of the Area between Dike 2 and the SDA

The topography between Dike 2 and the SDA over which a breach flood would travel has a general downward slope toward the southwest side of the SDA. The surface is relatively smooth, in the sense that it does not have rock outcrops or other severe breaks. However, it does have an undulating nonuniform pattern of mild peaks and valleys typical of desert land in Southeastern Idaho. Although there are no distinct drainage channels in evidence, there is a general depression, or series of depressions, along the south side of the access road that forms a natural, direct flow path for a flood. In some locations, the flow path includes the road. The surface of this area, excluding the road surface, which is compacted gravel, appears to be sandy silt in texture and has a moderately thick cover of sagebrush and wild grasses.

A railroad embankment crosses this flow path about 1,800-ft northeast of Dike 2, having an alignment approximately perpendicular to the flow path. The embankment rises 6 to 9 ft above the natural ground surface at this location and has a 2-ft box culvert to accommodate drainage from one side to the other. The railroad embankment and high ground on the east and west sides of the flow path leading to the embankment form a small natural detention basin that extends back to Dike 2 during a flood. This area is outlined and shaded in Figure 1-5.

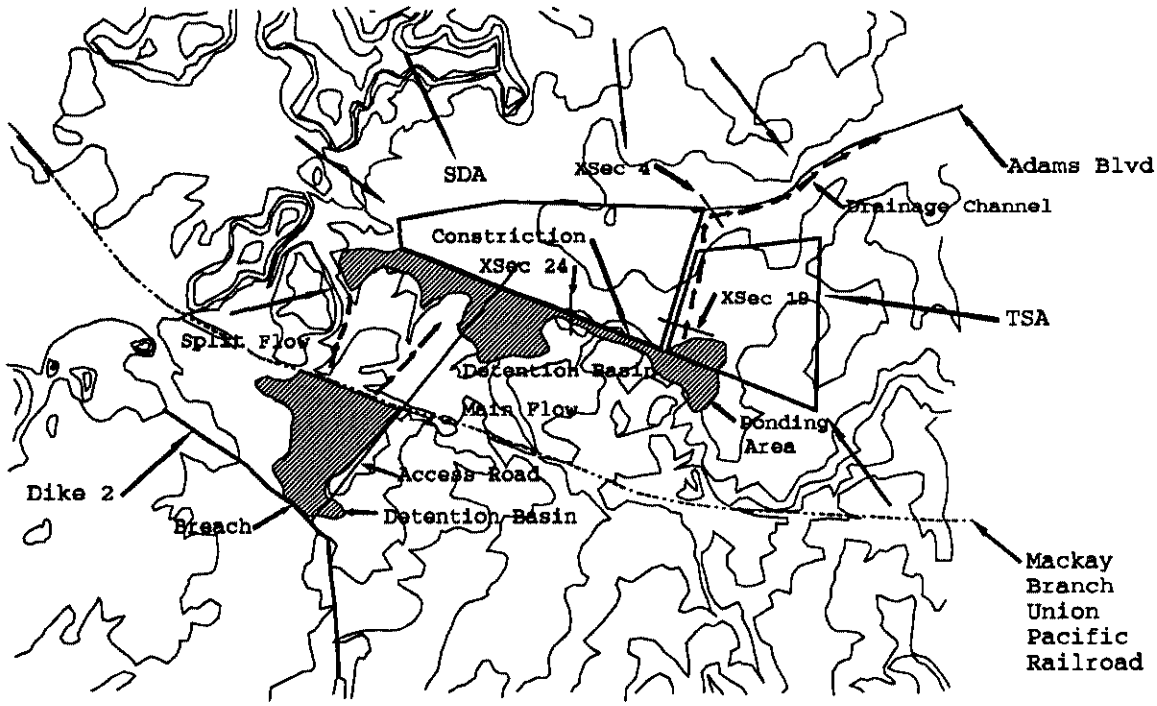

Figure 1-5 Flow paths and ponding areas near the SDA and the TSA

On the northeast side of the railroad embankment, two approximately parallel gullies with relatively steep slopes provide two paths, about 1200 and 1400 ft long, for flows that overtop the railroad embankment. These split flow paths are indicated in Figure 1-5. At the lower end of these gullies there is a relatively flat area that extends several hundred feet north to the SDA berm and continues along the southwest side of the berm for almost its full length. This low, relatively flat area would be another small detention basin for flood flows emanating from a breach in Dike 2. A high ridge on the east end of this low area, in close proximity to the southeast corner of the SDA, would impose a severe constriction to flood flows. This would be the outlet for the detention basin, which is outlined and shaded in Figure 1-5.

1.2.6 Critical Locations at the SDA for Potential Flooding

One of the critical points at which overtopping of the SDA berm may occur coincides with the location of the constriction just described. The top-of-berm elevation at the constriction and for a short distance upstream (northwest) on the top of the berm is 5013.6 ft above msl. This is lower than any other point on the berm to the northwest, which is part of the detention basin perimeter. As water rises in the basin because of the constriction, this is

one of the first places it would overtop the berm.

The access road into the SDA on the southwest side is another critical location, because the top-of-berm elevation at this location is only 0.1 ft higher than the constriction. However, the elevation of the top of the berm on either side of the crossover is higher than on the crossover itself, so the amount of overtopping would be small unless the water level rose substantially.

If the flood water level in the detention basin described on the southwest side of the SDA rose above 5012.5 ft above msl, a small amount of flow would pass around the west end of the SDA and into the low areas to the north of the SDA. Elevation at the bottom of a saddle in the west-end access road about 200 ft west of the SDA berm is 5012.5 ft above msl is the elevation would be very small because the potential flow cross section at the west end is quite limited. Flooding along the north side of the SDA or the potential for overtopping of the berm on the north side would not be a problem. Even if the outflow around the west end were sufficient to fill the low areas on the north side of the SDA, the excess water would drain toward the east past the northeast corner of the SDA and into the drainage channel at that end.

1.2.7 Drainage Characteristics in the Vicinity of the TSA

At the southeast corner of the SDA in the area immediately south of the TSA there is another low area that would provide a very limited amount of detention storage for a flood flow. After this area is filled, which would happen quickly, the path of a flood would be north between the SDA and the TSA. The path would lead along the east embankment of the SDA to the inlet of the drainage channel near Adams Boulevard.

The top of the SDA berm is lower along this side, varying from 5012.9 ft above msl at the southeast corner to about 5010.4 ft above msl at Adams Boulevard (access road). There is a flat grassy area about 50 ft wide along the outside toe of the SDA berm that would offer relatively low resistance to a flood flow if it is maintained in its present trimmed condition. On the TSA (east) side of this grassy area there is a paved barrel storage pad, with elevations of the pad varying from 5013.2 to 5014.8 ft above msl, that would constrict the flow to the 50-ft width for part of the distance. This storage area begins about 100 ft north of the southeast corner of the SDA and extends approximately another 300 ft north along the flow path. Beyond this storage area to the north the ground surface generally is as low or lower than the grassy area next to the berm, so a flood flow could spread out over a wider area.

There are two narrow areas of low elevation within the TSA that would permit small portions of high flood flows to pass through the TSA to the north and into the drainage channel next to Adams Boulevard. If the water surface elevation exceeds 5011.7 ft above msl at the southeast corner of the SDA and the ponding area south of the TSA, a small amount of

flow would pass through a low area on the east side of the barrel storage pad, crossing over the access roads at each end as it travells north. If the water surface elevation exceeds 5012.1 ft above msl south of the TSA, a small amount of flow would also travel north on the east side of the covered (inflated roof) storage area over a narrow strip of land surface between this area and a maintenance building immediately east of it.

1.2.8 Drainage Conditions East of the SDA along Adams Boulevard.

The inlet to the drainage channel located at the intersection of the SDA berm and Adams Boulevard is constructed of four 3 x 4.75-ft oval-shaped culverts. Because of the high skew angle (about 60 degrees) of the entrance to these culverts, this inlet will be inefficient for transmitting flood flows. The effective area of the culvert openings is so small because of the high skew angle. Therefore, there would be a high energy loss and a backwater effect on a flood flow entering this inlet from the flow path along the SDA berm.

The drainage channel from this culvert east is about 20 ft wide and 5 to 7 ft deep. The channel is has steep, almost vertical side slopes, and a sand and gravel bottom with a few weeds. There are extensive paved areas on both sides of the channel from the inlet culvert to the security facilities, approximately 1000 ft to the east. There are also several buildings and some fences on both sides of the channel in this area. Most of the buildings are located 100 to 200 ft back from the channel. There is a wooden bridge and a concrete bridge across the channel 400 and 550 ft east of the inlet culvert, respectively. From the security facilities east, the drainage channel parallels Adams Boulevard on the south side for several hundred feet, crosses to the north side through a culvert, continues generally in a northeast direction into the desert, and eventually leads back to the Big Lost River.

2 INEL DIVERSION AREA FLOW SYSTEM MODEL

The INEL Diversion Area Flow System Model was designed to simulate surface reservoir flow in the Diversion Area during periods of diverted flows from the Big Lost River (see Figure 1-2). The governing equation for which the model is based upon is the continuity of mass principle for open reservoir flow. Simply stated, this principle, as applied to the model, accounts for all water flowing in and out of the Diversion Area and the water stored in the spreading areas. Inflow for the model includes water diverted from the Big Lost River through the diversion channel, flow through the bypass swales west of the diversion dam, and precipitation. Model definition for outflow of water from the Diversion Area is ultimately based upon infiltration and evaporation because the connecting channel between Spreading Areas A and B and the Dike 3 weir only transport water from one spreading area to another. Storage is defined as the volume of water in each spreading area at a point in time.

Program Diversion Area FLOW (DAFLOW) was constructed to numerically simulate the INEL Diversion Area Flow System Model. It is a transient one-dimensional code designed to determine the water surface elevations in the spreading areas at a specific point in time.

2.1 Flow Parameters for the INEL Diversion Area Flow System Model

Flow parameters for the INEL Diversion Area Flow System Model are the physical characteristics of the Diversion Area that directly affect the inflow, outflow, and storage of the flow model. These parameters include

- Surface area and storage of the Diversion Area
- Physical flow characteristics of the connecting channel between Spreading Sreas A and B
- Physical flow characteristics of the Dike 3 weir
- Infiltration, evaporation, and precipitation rates in the INEL Diversion Area
- Diversion of the Big Lost River into the spreading areas.

Whether the above parameters are variables or constants is based upon available field data. The spreading area's surface area and volume values are functions of water surface elevation. The connecting channel was recently surveyed and from which an approximate hydraulic equivalent of constant cross sectional area and slope was derived. Flow in the connecting channel is a function of the water surface elevations in Spreading Areas A and B. Flow in the Dike 3 weir is a function of the water surface elevation in Spreading Area D.

For this modeling effort, evaporation, infiltration, and precipitation rates are constants because of a lack of detailed field data. Diversion rates from the Big Lost River are a function of time. Detailed diversion rates recorded during the 1965 flood were used in conjunction with a simulation of the diversion rates to the spreading areas that would result from a Mackay Dam failure.

2.1.1 Surface Area and Storage of the INEL Diversion Area

As discussed in Section 1.2, the Diversion Area is a cascade reservoir system with three definable reservoirs. The first reservoir is Spreading Area A; the second is the combination of Spreading Areas B, C, and D; and the third is the Offsite Spreading Area. The INEL Diversion Area Flow System Model evaluates each reservoir individually by employing the continuity of mass principle to determine the reservoir's water surface elevation at a point in time. For each reservoir, in a given length of time, the sum of the reservoir outflow and change in storage is equal to the reservoir inflow. The water surface area of a reservoir is required to determine the contribution of precipitation to reservoir inflow and evaporation and infiltration to reservoir outflow. Because at any point in time, outflow rarely equals inflow, there is a resultant storage in the reservoir. Both reservoir water surface area and storage can be defined as a function of a single variable, elevation. For any water surface elevation in a reservoir, there corresponds a unique value of water surface area and storage.

Tables defining water surface elevation compared to water surface area and storage for the three reservoirs are required for the INEL Diversion Area Flow System Model. The tables were created by first digitizing isobeths on a 10-ft interval contour map (AEC, Contract AT(10-1)-12, 1949) for Spreading Areas A through D and on a 20-ft interval contour map (USGS, Big Southern Butte, 1972) for the Offsite Spreading Area. Gridding software (Surfer, Golden Software Inc., 1988) was then employed using the Kriging method from which the surface areas and volumes could be numerically integrated. Table 2-1, 2-2, and 2-3 contain the water surface area and storage values vs. elevation (msl) for Spreading Area A; Spreading Areas B, C, and D; and the Offsite Spreading Area, respectively.

Table 2-1 Elevation (above msl) compared to water surface area and storage for Spreading Area A

Elevation (ft)	Water Surface Area (ft^2)	Storage (ft^3)	Elevation (ft)	Water Surface Area (ft^2)	Storage (ft^3)
5032.0	1.6200E+02	1.1700E+01	5046.0	2.4071E+07	1.5078E+08
5033.0	4.3742E+04	9.4629E+03	5047.0	2.6860E+07	1.7622E+08
5034.0	2.7506E+05	1.3875E+05	5048.0	3.1219E+07	2.0494E+08
5035.0	8.2032E+05	6.6357E+05	5049.0	3.8349E+07	2.3941E+08
5036.0	2.0297E+06	2.0021E+06	5050.0	4.7688E+07	2.8266E+08
5037.0	4.4890E+06	5.1376E+06	5051.0	6.5150E+07	3.3792E+08
5038.0	8.2067E+06	1.1340E+07	5052.0	9.5933E+07	4.1818E+08
5039.0	1.2461E+07	2.1561E+07	5053.0	1.2986E+08	5.3275E+08
5040.0	1.4685E+07	3.5295E+07	5054.0	1.5670E+08	6.7617E+08
5041.0	1.6275E+07	5.0801E+07	5055.0	1.8387E+08	8.4629E+08
5042.0	1.7737E+07	6.7812E+07	5056.0	2.1458E+08	1.0452E+09
5043.0	1.9221E+07	8.6296E+07	5057.0	2.4826E+08	1.2765E+09
5044.0	2.0688E+07	1.0624E+08	5058.0	2.9175E+08	1.5444E+09
5045.0	2.2187E+07	1.2765E+08	5059.0	3.5225E+08	1.8424E+09

Table 2-2 Elevation (above msl) compared to combined water surface area and storage for Spreading Areas B, C, and D

Elevation (ft)	Water Surface Area (ft^2)	Storage (ft^3)	Elevation (ft)	Water Surface Area (ft^2)	Storage (ft^3)
5014.0	2.2974E+03	1.0260E+02	5034.0	5.3881E+07	4.0642E+08
5015.0	3.7804E+04	7.3638E+03	5035.0	5.6899E+07	4.6175E+08
5016.0	2.5574E+05	1.2823E+05	5036.0	6.0158E+07	5.2024E+08
5017.0	8.4188E+05	6.5761E+05	5037.0	6.4117E+07	5.8230E+08
5018.0	2.0207E+06	2.0164E+06	5038.0	7.0819E+07	6.4919E+08
5019.0	4.0748E+06	5.0063E+06	5039.0	8.1875E+07	7.2481E+08
5020.0	6.0175E+06	1.0105E+07	5040.0	9.1293E+07	8.1252E+08
5021.0	7.8435E+06	1.7007E+07	5041.0	9.5831E+07	9.0618E+08
5022.0	1.0103E+07	2.5987E+07	5042.0	9.9390E+07	1.0039E+09
5023.0	1.2484E+07	3.7273E+07	5043.0	1.0260E+08	1.1049E+09
5024.0	1.5060E+07	5.0978E+07	5044.0	1.0557E+08	1.2088E+09
5025.0	1.7992E+07	6.7447E+07	5045.0	1.0847E+08	1.3157E+09
5026.0	2.1457E+07	8.7132E+07	5046.0	1.1200E+08	1.4259E+09
5027.0	2.5813E+07	1.1077E+08	5047.0	1.1757E+08	1.5407E+09
5028.0	3.1473E+07	1.3932E+08	5048.0	1.2585E+08	1.6621E+09
5029.0	3.7646E+07	1.7367E+08	5049.0	1.3666E+08	1.7927E+09
5030.0	4.2107E+07	2.1374E+08	5050.0	1.4517E+08	1.9341E+09
5031.0	4.5359E+07	2.5750E+08	5051.0	1.5198E+08	2.0829E+09
5032.0	4.8241E+07	3.0434E+08	5052.0	1.5858E+08	2.2359E+09
5033.0	5.1023E+07	3.5398E+08	5053.0	1.6518E+08	2.3889E+09

Table 2-3 Elevation (above msl) compared to water surface area and storage for the Offsite Spreading Area

Elevation (ft)	Water Surface Area (ft^2)	Storage (ft^3)	Elevation (ft)	Water Surface Area (ft^2)	Storage (ft^3)
5019.0	1.2089E+02	2.6222E+01	5037.0	1.1040E+07	7.0560E+07
5020.0	9.4831E+02	2.9283E+02	5038.0	3.0650E+07	8.2060E+07
5021.0	4.1092E+03	2.2856E+03	5039.0	7.7050E+07	1.1412E+08
5022.0	1.1602E+04	9.8034E+03	5040.0	8.2680E+07	1.9420E+08
5023.0	2.3151E+04	2.6842E+04	5041.0	8.6160E+07	2.7910E+08
5024.0	3.8779E+04	5.7458E+04	5042.0	8.9120E+07	3.6670E+08
5025.0	5.9641E+04	1.0616E+05	5043.0	9.1430E+07	4.5660E+08
5026.0	8.8865E+04	1.7961E+05	5044.0	9.3530E+07	5.4920E+08
5027.0	1.2781E+05	2.8713E+05	5045.0	9.5540E+07	6.4380E+08
5028.0	1.6612E+06	4.3846E+05	5046.0	9.7340E+07	7.4040E+08
5029.0	5.5472E+06	2.3553E+06	5047.0	9.9020E+07	8.3870E+08
5030.0	6.6514E+06	8.5560E+06	5048.0	1.0120E+08	9.3860E+08
5031.0	7.3403E+06	1.5550E+07	5049.0	1.0460E+08	1.0400E+09
5032.0	7.9813E+06	2.3230E+07	5050.0	1.0660E+08	1.1430E+09
5033.0	8.5774E+06	3.1510E+07	5051.0	1.0860E+08	1.2530E+09
5034.0	9.1563E+06	4.0330E+07	5052.0	1.1060E+08	1.3630E+09
5035.0	9.7531E+06	4.9700E+07	5053.0	1.1260E+08	1.4730E+09
5036.0	1.0380E+07	5.9850E+07			

2.1.2 Physical Flow Characteristics of the Connecting Channel

The connecting channel between Spreading Areas A and B is located approximately 1-mi west of the SDA (see Figure 2-1). It was excavated from an existing natural channel in 1958 as part of a flood-control project on the Big Lost River within the INEL. The channel was modified in 1987 to increase flow capacity.

Physical flow characteristics of the Connecting Channel are required for the INEL Diversion Area Flow System Model so that a flow relation between spreading areas A and B can be established. Morrison Knudsen - Fergusen at Idaho was contracted to survey the Connecting Channel. The survey included twenty-two cross sections with location and elevation measurements of .01 ft accuracy. Figure 2-1 shows the location of the Connecting Channel between spreading areas A and B with the orientation and locations of cross sections 1 - 22.

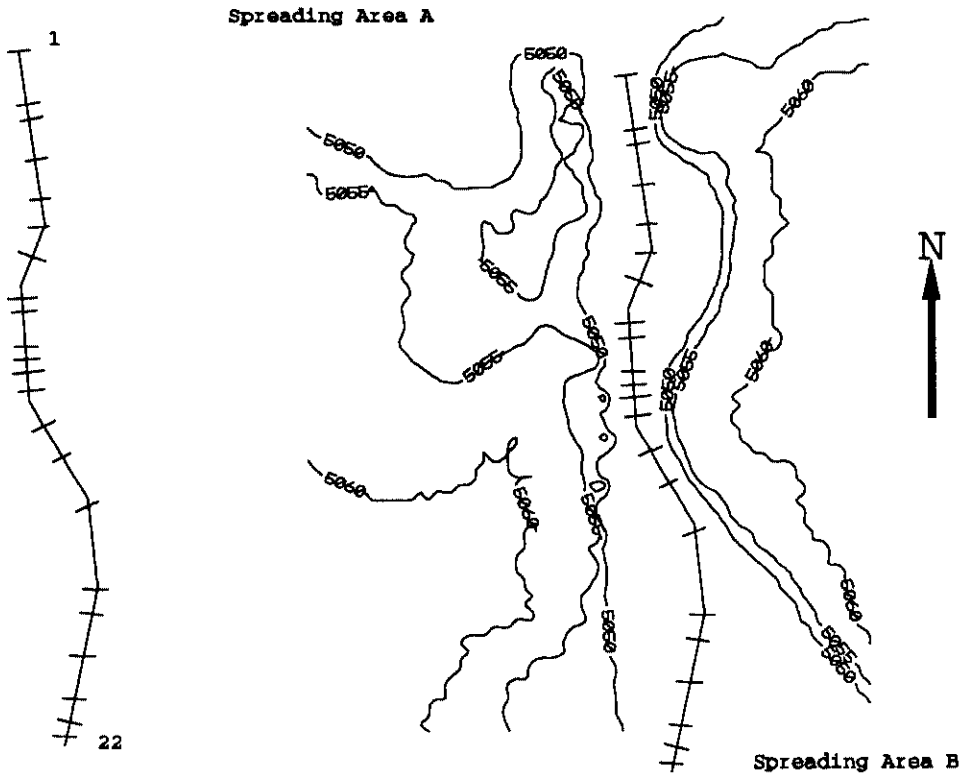

Figure 2-1 Location and orientation of the connecting channel and surveyed cross sections

A three-dimensional representation of the connecting channel is shown in Figure 2-2. It was created by combining the survey data with the digitized data from the 10-ft contour map. The elevation aspect (normal to the north-east plane) has been magnified by a factor of 10 to show the channel more clearly.

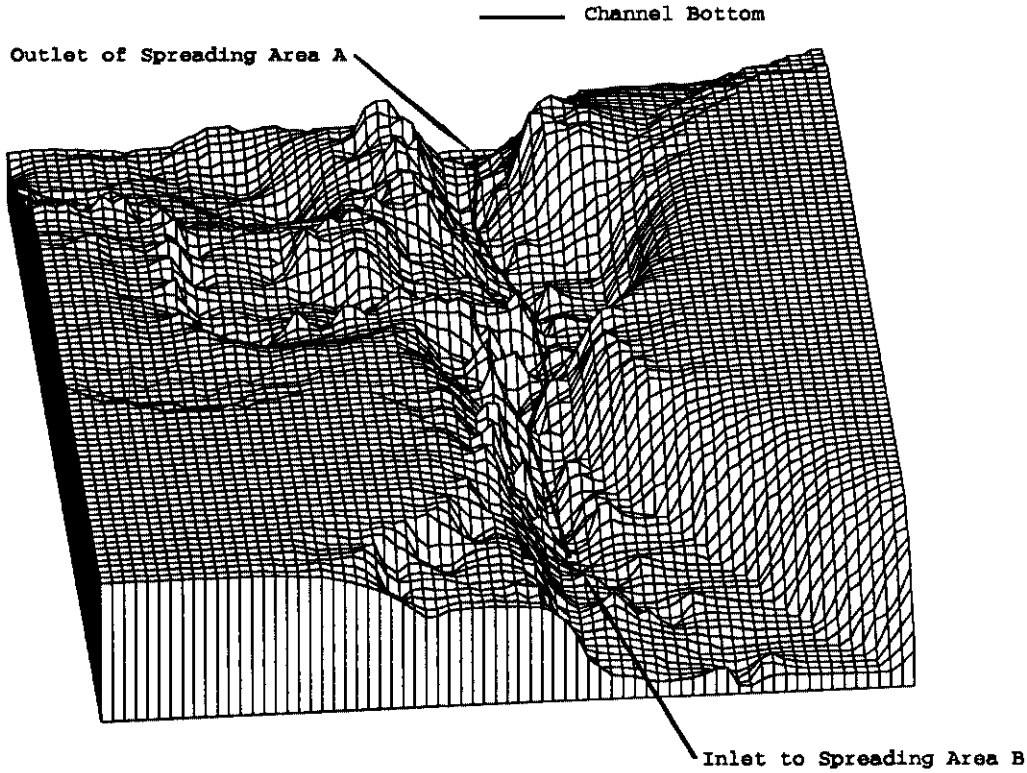

Figure 2-2 Three-dimensional view of the connecting channel

By personal observation, the Connecting Channel surface is composed mainly of fractured rock and loose boulders interspersed with areas of sediment, gravel, grass, and sagebrush. The channel from cross sections 1 through 13 has walls of rough rock. The channel bottom in this area is strewn with boulders and contains some sediment and brush. The channel from cross sections 13 - 18 is wider and shallower than the previous area. The channel in this area is mostly sediment and brush with the channel walls consisting of loose rock and gravel. Loose boulders and rock walls make up most of the channel from cross sections 18 through 22. Figures 2-3 through 2-5 show the geometric configuration of the connecting channel cross sections.

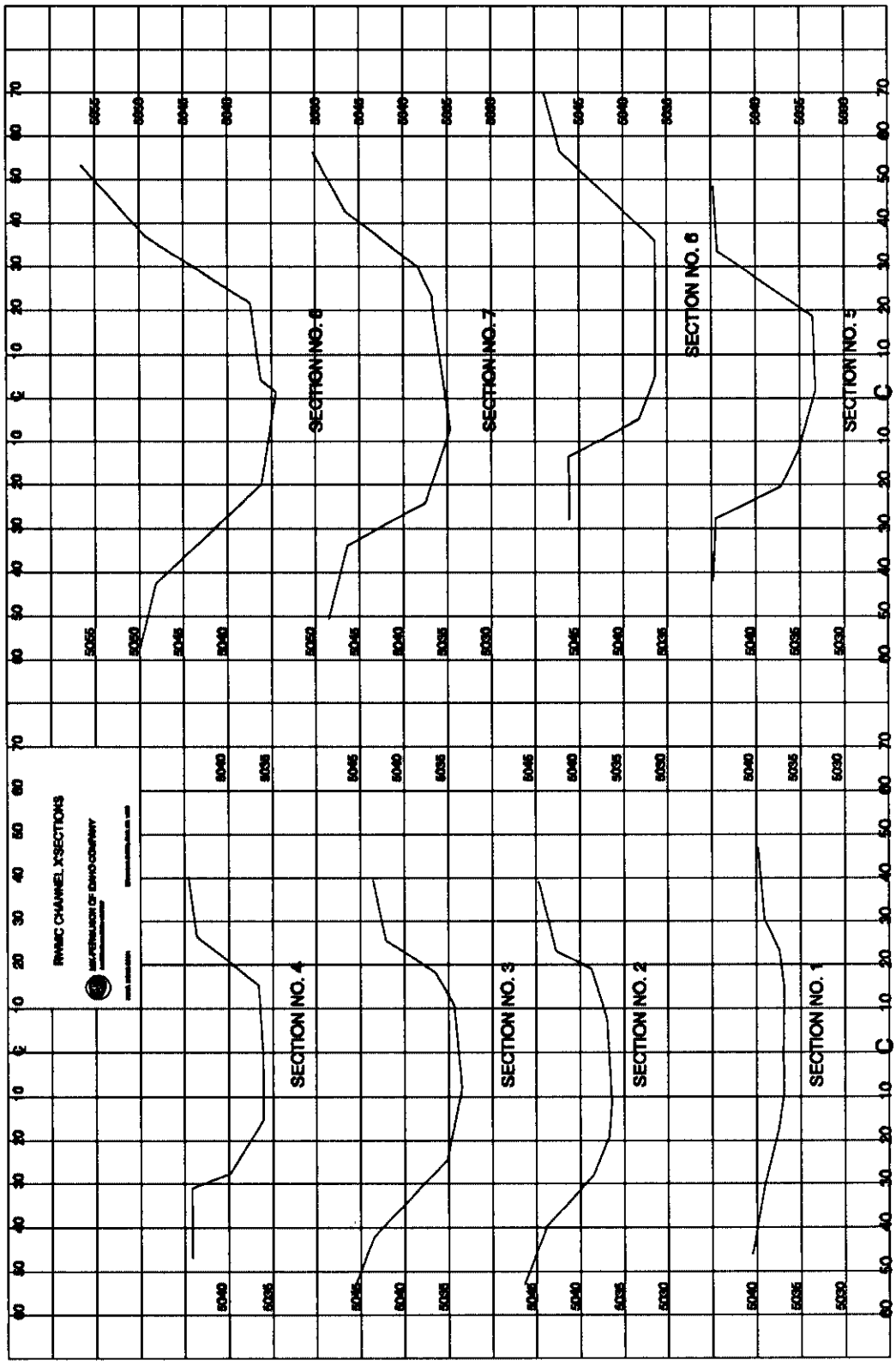

Figure 2-3 Geometric configuration of cross sections 1 through 8

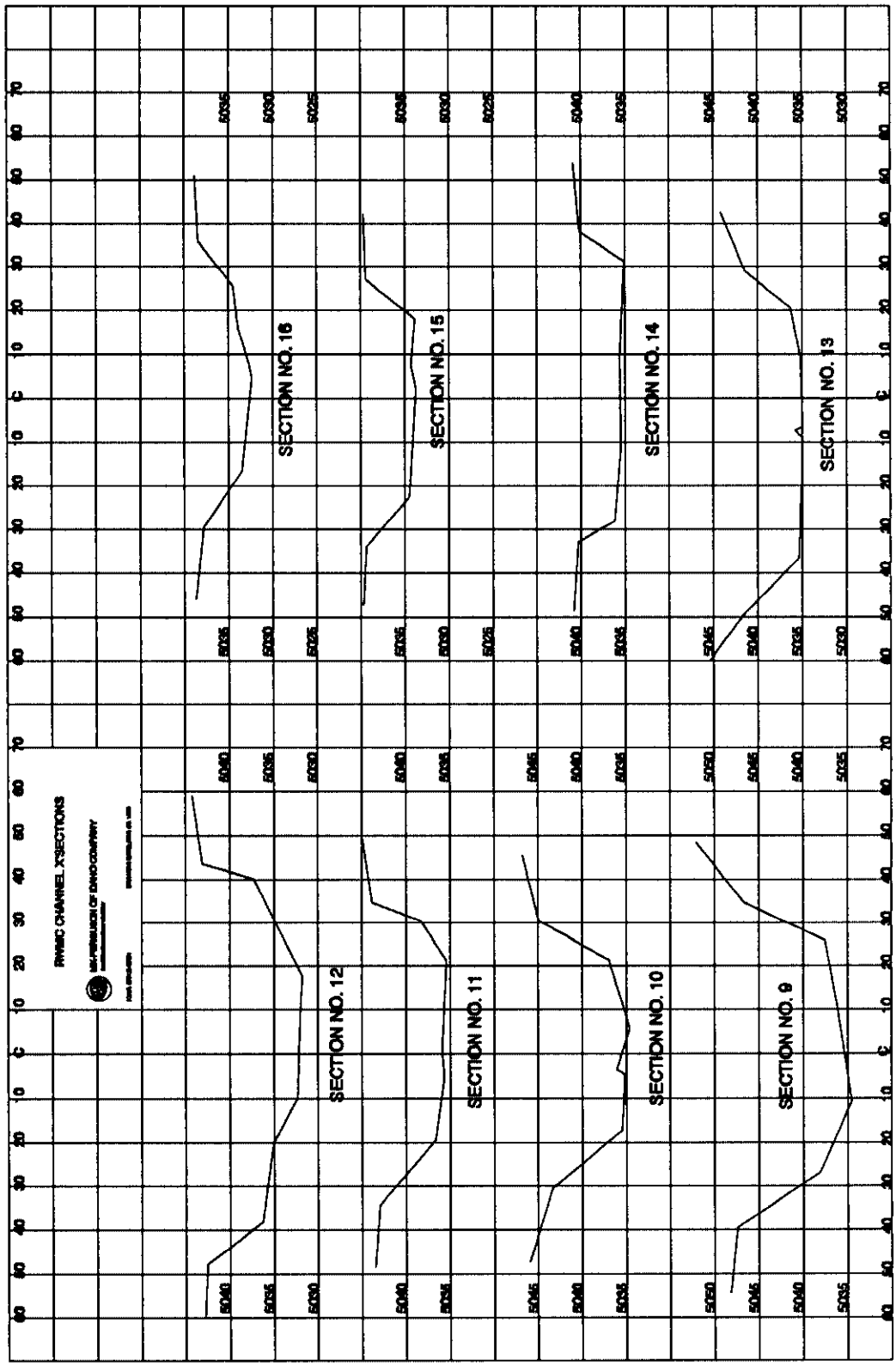

Figure 2-4 Geometric configuration of cross sections 9 through 16

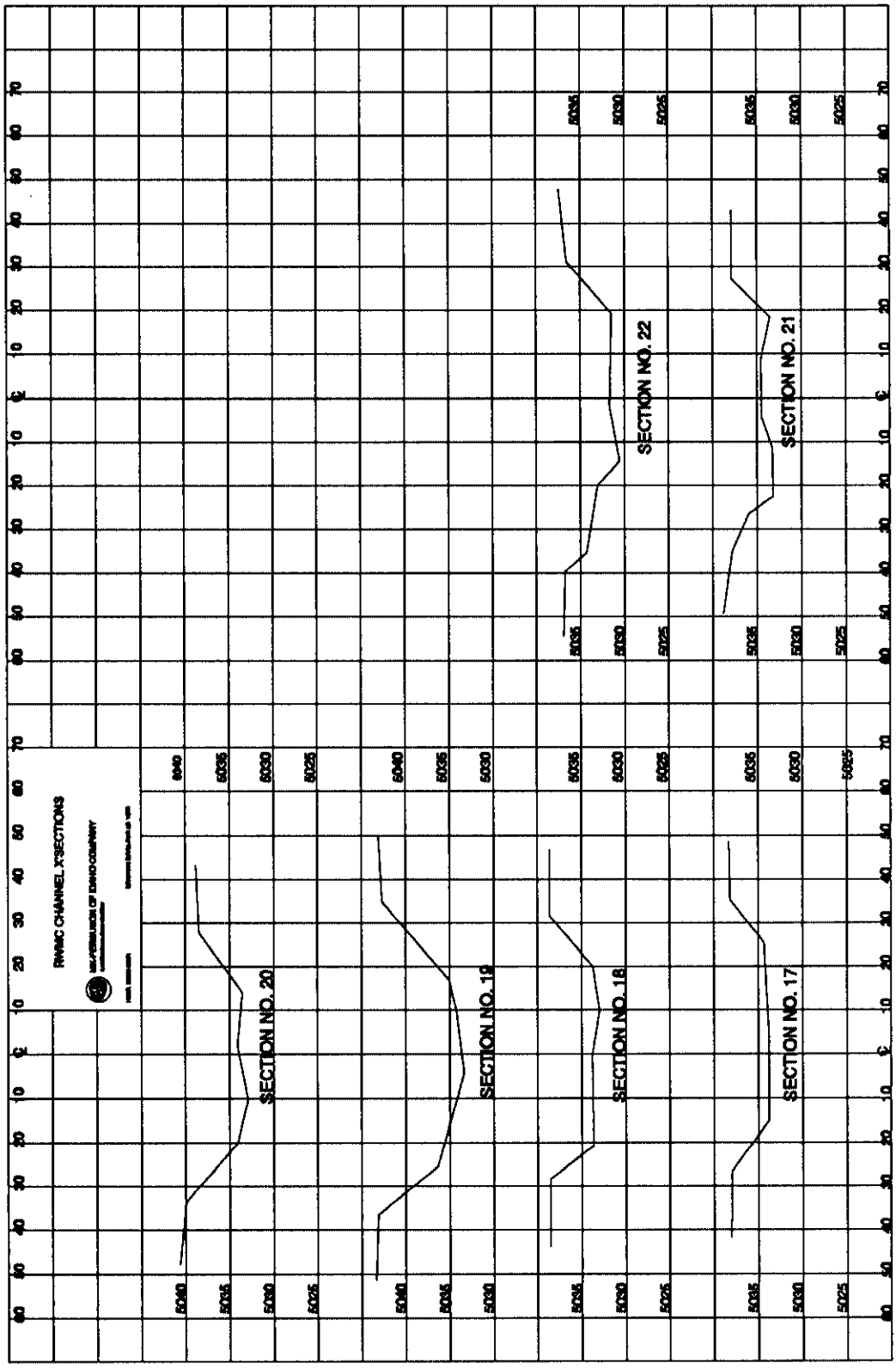

Figure 2-5 Geometric configuration of cross sections 17 through 22

Water begins to flow in the connecting channel when the water surface elevation in Spreading Area A reaches 5036.85 ft above msl. The limiting slope in the channel appears from cross sections 1 through 6. From cross section 6 on down the channel, the slope is considerably steeper. The elevation of the connecting channel bottom compared to the position in the channel is illustrated in Figure 2-6.

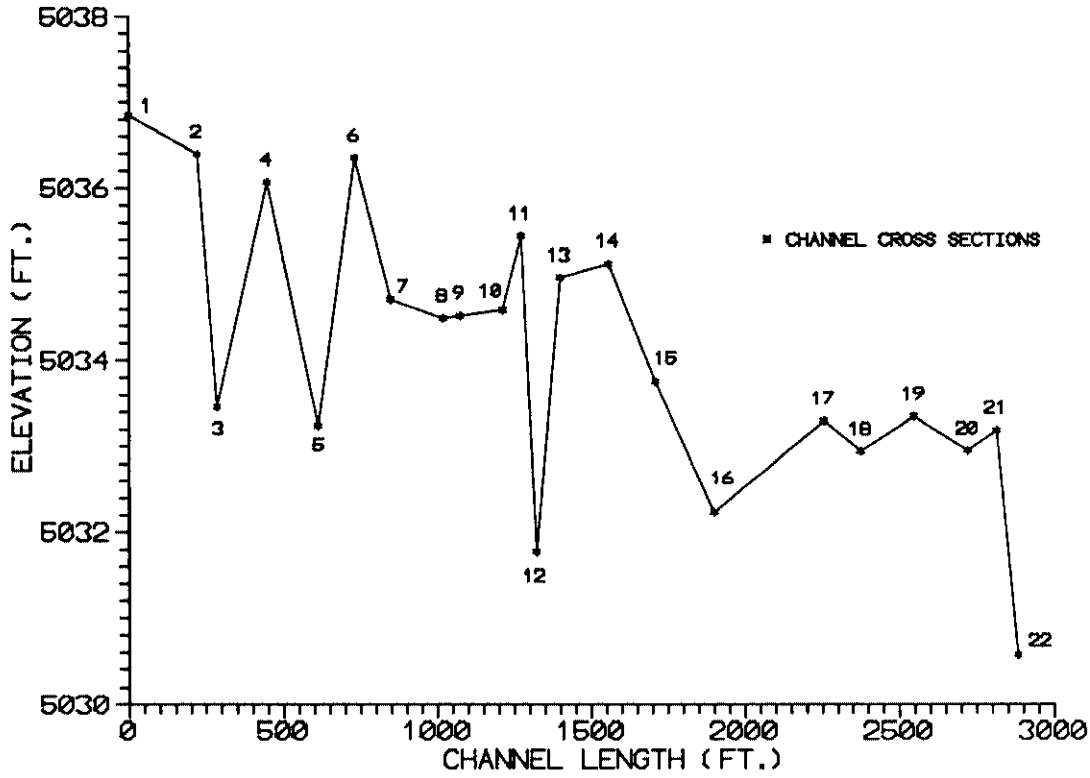

Figure 2-6 Connecting channel bottom elevation compared to channel position

There are areas in the channel where water will have to fill voids before there is flow. Referring to Figure 2-6, an area approximately 4 ft deep will be filled between cross sections 11 and 14. It is difficult to estimate how areas of high and low points will affect the channel flow. For the INEL Diversion Area Flow System Model, a hydraulic equivalent of constant cross sectional area and slope was estimated to simulate the connecting channel.

2.1.3 Physical Flow Characteristics of the Dike 3 Weir

Dike 3 is located at the southern end of Spreading Area D (see Figure 1-2). The Dike 3 weir is located approximately 1000 ft west of the east end of Dike 3. When the spreading areas are nearly full, water would flow over the weir crest into the Offsite Spreading Area. This would occur when the water surface elevation in the second reservoir (Spreading Areas

B, C, and D) reached 5038.6 ft above msl. The dike would be overtopped when the water surface elevation reached 5040.4 ft above msl. At this point, the maximum flow in the weir is 800 ft^3/s. The crest of the weir is made of a corrugated aluminum sheet with the sides of the packed earth and rock of Dike 3. As of 1990, water has never flowed over the weir's crest.

For the INEL Diversion Area Flow System Model, a hydraulic equivalent of the Dike 3 weir was calculated based upon the maximum volumetric flow rate, 800 ft^3/s, and the 1.8 ft weir height. The equivalent length for a rectangular weir is 96.2 ft The equation for volumetric flow and the geometry of the weir are discussed in Section 2.2.1.

2.1.4 Infiltration, Evaporation, and Precipitation rates in the INEL Diversion Area

Infiltration and evaporation are ultimately responsible for the total outflow of water in from the Diversion Area. Precipitation, in the form of rain and snow, is part of the inflow into the Diversion Area. These three parameters are used to calculate volumetric flow rates per unit area, which reduces to units of unit depth per unit length of time. The amount of inflow or outflow of these parameters is a function of water surface area because they act normal to the plane of the water surface. Therefore, these parameters are indirectly functions of water surface elevation for each of the three reservoirs.

Infiltration is the flow of water into the ground through the earth's surface by the force of gravity, surface tension, and capillarity (Viessman et al., 1977). The rate at which water infiltrates is influenced by the density of the vegetation cover, temperature, soil water content and quality, and the physical properties of the soil. Infiltration rates in ponded areas, as considered in this case, are greatly affected by hydraulic pressure. Hydraulic pressure is a function of ponded water depth.

The floor of the Spreading Area A is sediment covered with grass and sagebrush. The floor in Spreading Area B is similar to that in Spreading Area A with the exception of several small exposed basalt ridges that would increase the infiltration rate (Barraclough et al., 1967). After the 1965 flood, several places in Spreading Area B were found where water caused small parts of the sediment floor to collapse into tubes or fractures in the basalt. The largest hole found was 2.5 ft in diameter at the top, 6 ft in diameter at the bottom, and 13 ft deep. There were other holes ranging from 3 to 10 ft deep and from 2 to 6 ft in diameter. Obviously, a considerable amount of water drained into these holes. The floors of spreading areas C ,D, and the Offsite Spreading Area are similar to the floor of Spreading Area B.

Infiltration rates were measured in the spreading areas in October 1965 (Barraclough et al., 1967), which was well after the flow began in the Diversion Area on June 8, 1965. Spreading Areas A and B were measured with infiltration rates of 0.71 and 2.3 ft/day for Spreading Areas A and B, respectively. Because water had been ponded in these areas for 4 months, it is doubtful the infiltration rates were the same in October as they were in June

when the soil was very dry. No measurements were taken for Spreading Area C. Spreading Area D and the Offsite Spreading Area did not contain any water, and therefore, no measurements were taken. Spreading areas C and D and the Offsite Spreading Area are assumed to have a similar infiltration rate as Spreading Area B.

Evaporation of the ponded water is highly variable with temperature and humidity. Temperature and humidity vary greatly between night and day, with varying weather patterns, and on a seasonal basis. Pan evaporation measurements were conducted in September and October 1965 and were found to be 0.017 and 0.014 ft./day respectively (Barraclough et al., 1967). Evaporation rates were two orders of magnitude less than the measured infiltration rate in Spreading Area B.

Average annual precipitation in the Diversion Area has not been measured. However, average annual precipitation in the Central Facilities Area (CFA), which is about 5 miles northeast of RWMC (see Figure 1-1), is 8.71 in./y (Robertson et al, 1974). May and June are the wettest months in the CFA vicinity with an average of 1.2 in./mo. This translates into 0.0035 ft/d, which is even more insignificant than evaporation when used in the model.

2.1.5 Diversion of the Big Lost River into the Spreading Areas

The diversion channel (see Figure 1-2) was excavated in 1958 (Bennet, 1986) through several basalt ridges and intervening surficial sedimentary deposits to connect the Big Lost River with the spreading areas. Water is diverted into the diversion channel by a earthen dam across the Big Lost River. The diversion dam is continuous with Dike 1. Two 6-ft diameter corrugated metal culverts permit a maximum flow of 900 ft^3/s through the dam back into the river. Flow in the river below the dam is then regulated by the gates in the pipes to a maximum of 900 ft^3/s. During high river flows in excess of 900 ft^3/s, water flows into the diversion channel and then into Spreading Area A. Flow in the channel is uncontrolled at discharges that exceed the capacity of the pipes. In some instances, Big Lost River flow below 900 ft^3/s is not entirely diverted. Some water is allowed to flow down the river to provide some surface recharge and to help keep the channel clear of brush. The south dike of the diversion channel was modified in 1984 to increase flow capacity to 7200 ft^3/s (Bennet, 1986).

There is a recording-gauge station located on the diversion channel about 500 ft downstream from the diversion dam. Volumetric flow rates are available from the USGS for March 29, 1965, until the present.

2.2 INEL Diversion Area Flow System Model Program (DAFLOW)

An INEL Diversion Area Flow System Model (DAFLOW) has been constructed to numerically simulate the INEL Diversion Area Flow System Model. The program calculates the water surface elevations of the spreading areas at a specific point in time, given a diversion channel flow history. The model is based upon the continuity of mass principle for open reservoir flow. A listing of DAFLOW is provided in Appendix A.

As discussed earlier, the Diversion Area can be divided into three reservoirs. DAFLOW applies the continuity mass principle to each reservoir individually. The program checks to see if each reservoir has a volume of water before determining the value of inflow and outflow of water. Iteration on the water surface elevation of each reservoir provides an elevation that will satisfy the continuity principle. Water surface elevations of the reservoirs are dependent upon one another. For example, the water surface elevation in Spreading Area A determines how much water flows through the connecting channel and, therefore, the water surface elevation in Spreading Area B.

The principle of continuity accounts for all water flowing in and out of a reservoir with the rate of change in the storage of the reservoir. For the first reservoir, inflow is defined as the sum of the diversion channel flow and the amount of precipitation that falls on Spreading Area A in a specific length of time. Outflow is defined as the sum of the connecting channel flow and the amount of infiltration and evaporation in Spreading Area A. Inflow for the second reservoir is defined as the sum of the connecting channel flow and the amount of precipitation that occurs in Spreading Areas B, C, and D. Outflow in the second reservoir is defined as infiltration, evaporation, flow out of the Dike 3 weir if the water surface elevation is 5038.6 ft above msl or higher, and possibly flow over Dike 3 in the case of the hypothetical Mackay Dam failure. Inflow for the third reservoir occurs when there is Dike 3 weir flow and possibly flow over Dike 3. Precipitation is only included if there is storage in the reservoir because the infiltration and evaporation rates are greater than the precipitation rate. Change in storage for the reservoirs is defined as the difference in storage for each reservoir for the given length of time.

2.2.1 Continuity of Mass Principle for Open Reservoir Flow

The continuity of mass principle for open reservoir flow is based upon the average rates of inflow, outflow, and storage (Linsley and Franzini, 1979). This principle is expressed in the storage equation

$$\bar{I}\Delta t - \Delta s = \bar{O}\Delta t \qquad (2\text{-}1)$$

where $\bar{I}$ and $\bar{O}$ are the average rates of inflow and outflow for the time interval Δt. Δs is the change in storage of the reservoir for Δt.

The average value assumption for the inflow and outflow rates requires that the water surface of the reservoir be nearly level. The occurrence of a level water surface is true in reservoirs where the storage of the reservoir is much larger than the amount of water that flows into and out of the reservoir over a sufficiently small length of time. This is because reservoirs tend to attenuate the transient effect of inflowing and outflowing water, as in the case of this study. For example, water flowing into Spreading Area A will increase from 2000 to 22,000 ft^3/s in approximately twenty eight hours for the hypothetical Mackay Dam failure (discussed in Section 2.3). At the point the maximum flow occurs, there will be approximately 217,000,000 ft^3 of water in the first reservoir. For a sufficiently small length of time, for example 1 hr, 57,000,000 ft^3 of water will be added to the reservoir. This will cause a 1.8-ft increase in the water surface elevation of the reservoir. Over a 1 hr period, this increase in elevation is small enough to assume that the water surface will remain level.

Discretizing Equation (2-1) forward in time and expressing the flows as averages, yields

$$\frac{I_n + I_{n+1}}{2} - \frac{O_n + O_{n+1}}{2} = \frac{S_{n+1} - S_n}{2} \qquad (2\text{-}2)$$

where

I_n = reservoir inflow at present time step

I_{n+1} = reservoir inflow at next time step

O_n = reservoir outflow at present time step

O_{n+1} = reservoir outflow at next time step

S_n = reservoir storage at present time step

S_{n+1} = reservoir storage at next time step.

This equation represents the reservoir storage rate in terms of the average difference in reservoir inflow and outflow. I_n, I_{n+1}, O_n, and S_n are known values whereas O_{n+1} and S_{n+1} are unknown. Because there is only one equation and two unknowns, Equation (2-2) has to be solved iteratively. All the variables in Equation (2-2) are functions of water surface elevation. Therefore, a value of water surface elevation will have to be found iteratively that will satisfy the equation.

Applying Equation (2-2) for the first reservoir, the terms in Equation (2-2) become

$$I_n = [Q_{DC} + A_A K_P]_n$$

$$I_{n+1} = [Q_{DC} + A_A K_P]_{n+1}$$

$$O_n = [Q_{AB} + A_A(K_{IA} + K_E)]_n$$

$$O_{n+1} = [Q_{AB} + A_A(K_{IA} + K_E)]_{n+1}$$

where

A_A = water surface area of Spreading Area A

K_P = precipitation rate Diversion Area

K_{IA} = infiltration rate of Spreading Area A

K_E = evaporation rate of Diversion Area

Q_{DC} = flow in Diversion Channel

Q_{AB} = flow in Connecting Channel

Applying Equation (2-2) for the second reservoir, the terms in Equation (2-2) become

$$I_n = [Q_{AB} + A_B K_P]_n$$
$$I_{n+1} = [Q_{AB} + A_B K_P]_{n+1}$$
$$O_n = [Q_W + A_B(K_{IB} + K_E)]_n$$
$$O_{n+1} = [Q_W + A_B(K_{IB} + K_E)]_{n+1}$$

where

A_B = combined water surface area of spreading areas B, C, and D

K_{IB} = infiltration rate of Spreading Area B

Q_W = flow in Dike 3 Weir

Applying Equation (2-2) for the third reservoir, the terms in Equation (2-2) become

$$I_n = [Q_W + A_O K_P]_n$$
$$I_{n+1} = [Q_W + A_O K_P]_{n+1}$$
$$O_n = [A_O(K_{IB} + K_E)]_n$$
$$O_{n+1} = [A_O(K_{IB} + K_E)]_{n+1}$$

where

A_O = water surface area of the Offsite Spreading Area.

The infiltration rate, K_{IB}, is the same for both the second and third reservoirs.

2.2.2 Determining Flow in the Connecting Channel

The connecting channel is an open channel that allows water to be transferred from Spreading Area A to Spreading Area B. An open channel is defined as a conduit with a free water surface. Because there is a reservoir upstream, flow in the connecting channel is assumed to be constant. This is a assumption based upon the Spreading Area A characteristic

of attenuating all diversion channel transients and the water surface elevation of Spreading Area A changing slowly over a relatively small time period. Constant flow is steady-state flow that has a constant mass flow rate. An open channel with constant flow has a hydraulic equivalent, for a given flow rate, that is of constant slope and cross section even though physically the channel is highly variable in both slope and cross section as is the connecting channel (see Section 2.1.2).

There are two types of constant flow possible in the connecting channel. The first is uniform flow that has constant average velocity and normal depth from free water surface to channel bottom. The second is defined as submerged flow. Submerged flow occurs when the surface of the downstream reservoir is higher than the bottom of the channel at the upstream reservoir. The depth of the water in a submerged channel is not constant; therefore, average velocity along the length of the channel is not constant.

2.2.2.1 Uniform Flow in an Open Channel

Figure 2-7 illustrates channel geometry for uniform flow of water in an open channel.

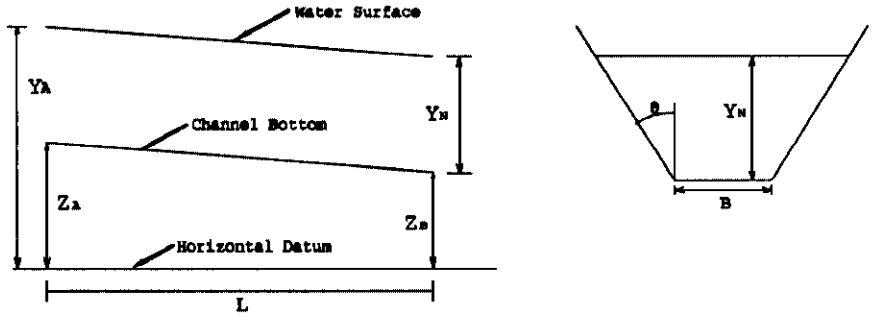

Figure 2-7 Geometry definition for uniform flow in an open channel

Z is the elevation of the channel bottom above an arbitrary horizontal datum where, in the case of the Connecting Channel , the horizontal datum is 0.0 ft above msl. Z_A and Z_B are the elevations of the channel bottom at the inlet and outlet, respectively. L is the length of the channel, Y_A is the elevation of the water surface at the inlet, and Y_N is the normal depth at which uniform flow will occur in an open channel. For uniform flow, the water surface in the channel is parallel to the channel bottom.

Several equations are used to calculate the rate of flow in an open channel. The Chézy equation (Linsley and Franzini, 1979) is

$$V = C(RS_0)^{\frac{1}{2}} \tag{2-3}$$

where V is the average flow velocity in the channel and C is the flow coefficient. R is the hydraulic radius and is expressed as

$$R = \frac{A}{P}$$

where A is the cross sectional area of the flow and P is the wetted perimeter. S_0 is the is the slope of the channel bottom and may be determined by

$$S_0 = \frac{Z_A - Z_B}{L} \quad .$$

In uniform flow, the slope of the channel bottom is equal to the slope of the channel's water surface. The slope used to simulate flow in the connecting channel was $6.834\ 10^{-4}$. Equation (2-3) is applicable when the channel slope is less than 0.10. With the mild slope of the Connecting Channel, the flow is subcritical (i.e., no hydraulic jumps). Therefore, the slope of the channel is always positive because water always flows down hill in subcritical flow.

The Chézy coefficient is the most commonly used flow coefficient for C in Equation 2.3 and is defined as

$$C = \frac{1.49}{n} R^{\frac{1}{6}}$$

where n is the roughness coefficient. If the roughness is not uniform across the channel width, an average value of n must be selected. An n value of 0.045 was selected for the Connecting Channel. This is an average value of n for the first six cross sections in the channel. The value of n was derived from Table 10-3 (Roberson and Crowe, 1985).

Substituting the Chézy coefficient into Equation 2-3 gives the Manning equation

$$V = \frac{1.49}{n} R^{\frac{2}{3}} S^{\frac{1}{2}} \quad . \tag{2-4}$$

Multiplying Equation 2-4 by the cross sectional area, A, yields the Manning equation for discharge

$$Q = \frac{1.49}{n} A R^{\frac{2}{3}} S^{\frac{1}{2}} \tag{2-5}$$

Equation 2-5 can be expressed in terms of channel geometry for the connecting channel. Referring to Figure 2-7, the discharge equation is

$$Q_{AB} = \frac{1.49}{n}\left[(Y_A - Z_A)\left(B + (Y_A - Z_A)\tan\theta\right)\right]^{\frac{5}{3}} \left[B + \frac{2(Y_A - Z_A)}{\cos\theta}\right]^{-\frac{2}{3}} \tag{2-6}$$

where Q_{AB} is the connecting channel discharge, Y_A is the water surface elevation in Spreading Area A, B is the width of the channel bottom, and θ is the angle from the vertical that defines the channel sides.

2.2.2.2 Submerged Flow in an Open Channel

Submerged flow occurs when the water surface downstream from the channel is high enough to reduce the discharge. Resistance to flow in the downstream part of the channel becomes sufficient to reduce the velocity, increase the flow depth, and cause a backwater effect in the channel (ISCO, 1981). Figure 2-8 illustrates the geometry of a submerged channel.

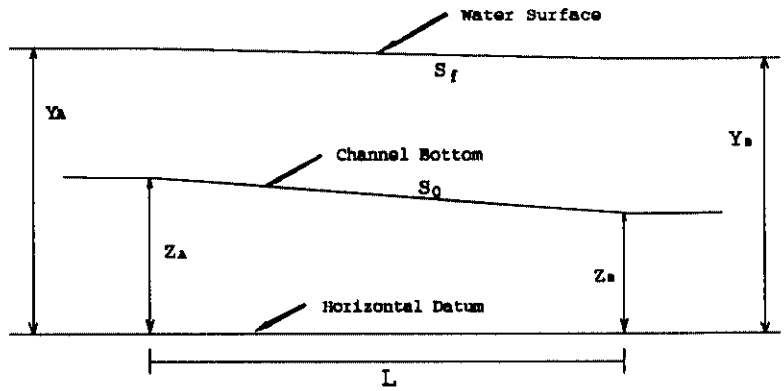

Figure 2-8 Geometry definition for submerged flow in an open channel

Submerged flow requires knowledge of the upstream and downstream channel depth. The ratio of the downstream depth to the upstream depth, expressed as a percentage, is

referred to as the submergence ratio. In most instances, discharge is determined by using submerged flow tables. This is because the equations governing submerged flow are nonlinear and difficult to solve. Because submerged flow tables for the connecting channel are not available, the governing equations were manipulated to derive a semi-analytical solution to incorporate into DAFLOW.

DAFLOW assumes steady-state flow over a time step. In a submerged channel under steady-state flow, the backwater effect resembles a standing wave because the water surface is no longer parallel to the channel bottom (see Figure 2-8). A wave is defined as a temporal (i.e., with respect to time) or spatial (i.e., with respect to distance) variation of flow or water surface (Chaudhry, 1979). In the connecting channel case, the wave is represented by a spatial variation that does not move relative to the channel. The standing wave in the connecting channel is a monoclinal wave (i.e., a wave having one rising limb).

The governing equations for transient channel flow are the St. Venant equations (Chaudhry, 1979). In one-dimensional spatial form, they are

$$\frac{\partial y}{\partial t} + V\frac{\partial y}{\partial x} + \frac{A}{B}\frac{\partial V}{\partial x} = 0 \qquad (2\text{-}7a)$$

$$g\frac{\partial y}{\partial x} + \frac{\partial V}{\partial t} + V\frac{\partial V}{\partial x} = g(S_0 - S_f) \qquad (2\text{-}7b)$$

where g is the gravity acceleration constant and S_f is the average slope of the water surface which may be computed using any formula for steady-state losses such as the Manning equation. This system of equations is nonlinear through the advection term of Equation 2-7b. The equation system must either be solved numerically or by transforming the equations into a more simple form.

Because, the connecting channel is being modeled with steady-state flow and a standing wave, the partial derivatives with respect to time terms go to zero.

$$V\frac{\partial y}{\partial x} + \frac{A}{B}\frac{\partial V}{\partial x} = 0 \qquad (2\text{-}8a)$$

$$g\frac{\partial y}{\partial x} + V\frac{\partial V}{\partial x} = g(S_0 - S_f) \qquad (2\text{-}8b)$$

To create a single linear equation out of Equation 2-8, multiply Equation 2-8a by V, Equation 2-8b by A, and divide Equation 2-8b by B.

$$V^2\frac{\partial y}{\partial x}+V\frac{A}{B}\frac{\partial V}{\partial x} = 0 \qquad (2\text{-}9a)$$

$$g\frac{A}{B}\frac{\partial y}{\partial x}+V\frac{A}{B}\frac{\partial V}{\partial x} = g\frac{A}{B}(S_0-S_f) \qquad \textbf{2.9b}$$

Subtracting Equation 2-9b from Equation 2-9a yields

$$\left(V^2-g\frac{A}{B}\right)\frac{dy}{dx} = -g\frac{A}{B}(S_0-S_f) \qquad (2\text{-}10)$$

The normal depth, Y_N, of the submerged channel varies with the length of the channel. However, the relationship between the normal depth and velocity is a constant. The connecting channel can be viewed as a control volume where mass is conserved (i.e., mass flow into the channel equals mass flow out of the channel). In mass flow rate terms, this can be expressed as

$$(\rho AV)_i = (\rho AV)_o$$

where ρ is density, i subscript refers to the inlet, and o subscript refers to the outlet. Because density is a constant in incompressible flow

$$A_iV_i = A_oV_o$$

or

$$\frac{A_i}{A_o} = \frac{V_i}{V_o} \quad .$$

The cross sectional area of the flow is

$$A = Y_N(B+2\tan\theta) \quad .$$

Therefore,

$$\frac{Y_{N_i}(B+2\tan\theta)}{Y_{N_o}(B+2\tan\theta)} = \frac{V_i}{V_o}$$

or

$$\frac{Y_{N_i}}{Y_{N_o}} = \frac{V_i}{V_o}$$

A, V, and S_f in Equation 2-10 are then average values of cross sectional flow area, velocity, and water surface slope for the submerged channel.

Equation 2-10 can be solved by separation of variables by rearranging into

$$\left(V^2 - g\frac{A}{B}\right)dy = -g\frac{A}{B}(s_0 - S_f)dx \tag{2-11}$$

Integrating the first term of Equation 2-11 through the channel depth and the second term by the effective length of the flow,

$$\left(V^2 - g\frac{A}{B}\right)\int_0^{Y_N} dy = -g\frac{A}{B}(s_0 - S_f)\int_0^{\frac{Y_A - Y_B}{S_f}} dx \tag{2-12}$$

yields

$$Y_N V^2 - g\frac{A}{B}Y_N = -g\frac{A}{B}\frac{S_0}{S_f}(Y_A - Y_B) + g\frac{A}{B}(Y_A - Y_B) \quad . \tag{2-13}$$

Solving Equation 2-13 for velocity, V,

$$V = \left[\frac{g\frac{A}{B}\left(Y_N + (Y_A - Y_B)\left(1 - \frac{S_0}{S_f}\right)\right)}{Y_N}\right]^{\frac{1}{2}} \tag{2-14}$$

and substituting the Manning equation for slope of the water surface,

$$S_f = \left(n\frac{V}{1.49}R^{-\frac{2}{3}}\right)^2$$

results in the final expression for the average velocity in a submerged channel

$$V = \left(\frac{g\frac{A}{B}\left\{ Y_N + (Y_A - Y_B)\left[1 - \frac{S_0}{\left(n\frac{V}{1.49}R^{-\frac{2}{3}} \right)^2} \right] \right\}}{Y_N} \right)^{\frac{1}{2}} \qquad (2\text{-}15)$$

Multiplying Equation 2-15 by the average cross sectional area of the flow, will give the total discharge of the channel. Equation 2-15 will have to be solved for iteratively. Newton's Method or a simple search method could be used to solve for velocity.

2.2.3 Dike 3 Flow

For the INEL Diversion Area Flow System Model, a hydraulic equivalent of the Dike 3 weir was calculated based upon the maximum volumetric flow rate, 800 ft^3/s, and the 1.8 ft weir height. Figure 2-9 illustrates the geometry for the equivalent rectangular weir.

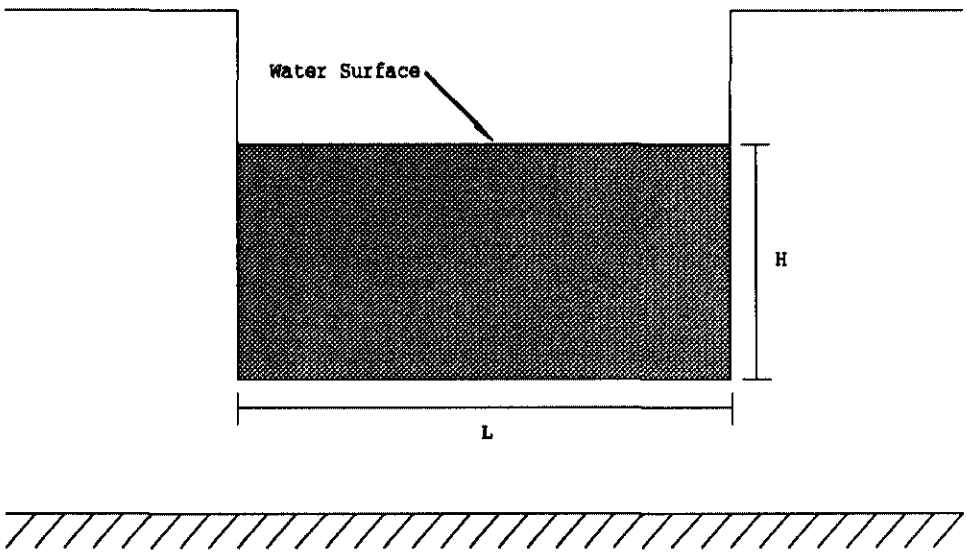

Figure 2.9 Rectangular Weir Geometry

The equation for volumetric flow through a rectangular weir (Roberson and Crowe, 1985) is

$$Q = \frac{2}{3} L\sqrt{2g}\, H^{\frac{3}{2}} \quad . \tag{2-16}$$

The equivalent length, L, for a rectangular weir is 96.2 ft. The flow height, H, varies from 0.0 to 1.8 ft, which corresponds to 5038.6 to 5040.4 ft above msl, respectively.

In the case of the hypothetical Mackay Dam failure, the water level in the second reservoir will probably crest the top of Dike 3. Dike 3 will then become a 3000 ft long broad crested weir. Flow through the weir will be neglected since the flow will be negligible compared to the flow over Dike 3. The equation for volumetric flow over a broad crested weir (Roberson and Crowe, 1985) is

$$Q = 0.544\, L\sqrt{2g}\, H^{\frac{3}{2}} \tag{2-17}$$

where L is the 3000 ft length of Dike 3 and H is the difference in water surface elevation of the second reservoir and the top of Dike 3, which is 5040.4 above msl.

2.3 Hypothetical Mackay Dam Failure Results by DAMBRK

Sections 2.3.1 and 2.3.2 were taken from Koslow and Van Haaften, (1986). Section 2.3.3 describes the inflow rates to the Diversion Area from the results of a DAMBRK simulation of a probable maximum flood PMF induced overtopping of the Mackay Dam.

2.3.1 Flood Routing Analysis

According to Koslow and Van Haaften (1986):

> Analysis of high-magnitude flooding caused by a dam failure relies on hydrodynamic theory to describe the dam-break wave and to propagate the wave downstream. Closed-form solutions do not exist for the partial differential equations of unsteady flow in open channels, so numerical techniques are employed to achieve solutions. The computer code DAMBRK uses one-dimensional hydraulic routing to solve the equations of continuity and momentum conservation. DAMBRK was developed by the National Weather Service (NWS), and represents the state-of-the-art in flood modeling. The code has been successfully tested against data from a number of actual dam failures, including the 1976 Teton Dam failure in eastern Idaho. The Teton flood analysis calculated flood flows within 5% of observed values (Fread, 1984).
>
> Three functional elements are involved in DAMBRK: description of the dam failure mode and initial conditions, computation of the time-varying flow

and water surface elevations at the breach, and routing of the flood through the downstream valley. These functions are accomplished using a number of input elements including beach description, reservoir inflow and storage characteristics, downstream frictional resistance, flow losses, and downstream channel geometry.

The river channel is described by dividing it into a number of reaches, each characterized by upstream and downstream valley cross sections and Manning's "n" values. The cross sections are measured normal to the direction of flow and are the basis for DAMBRK's one-dimensional description of the regular prismatic river channel. Each cross section is described by a table of valley width versus elevation. The valley surface roughness and frictional resistance to flow are represented by a table of Manning's "n" versus elevation estimated for each input reach. Manning's "n" values were estimated from field inspection and compared with USGS data and ranged from 0.030 to 0.060 (Harris, 1976). DAMBRK generates additional cross sections by linear interpolation between adjacent input sections. Time-dependent flows can be included at any reach to describe flows added to or lost from the flood.

DAMBRK has been designed to use cross-section data obtained from USGS topographic maps. For this analysis, 45 cross sections were read from the topographic maps. Of these, three were surveyed by the USGS within the INEL boundaries and agreed well with data from the topographic maps. Linear interpolation between these cross sections resulted in a total of 259 cross sections used in the DAMBRK analysis.

2.3.2 Mackay Dam Failure Analysis

According to Koslow and Van Haaften (1986):

The flood-routing analysis of a failure of Mackay Dam included resonable failure scenarios considering the condition of the dam and the geological and hydrological history of the area. These include failure during a seismic event, failure during normal operation, and failure during the most extreme flood event, PMF. The principal differences between these failures are the inflow to the reservoir and the reservoir water surface elevation at the time of failure. Because the dam was built for irrigation purposes, the reservoir waters are often maintained at the level of the spillway crest during the spring months. During normal operation, the reservoir water surface is expected to be at or below the level of the spillway crest (6,066.5 ft msl). During the PMF inflow, the water surface at the dam would rise to a level exceeding 6,077 ft above msl, overtopping the crest of the dam by more than 1 ft. Four cases have thus been included in this analysis:

1. Seismic failure of the dam, coincident with the 25-year recurrence interval flood
2. Hydraulic (piping) failure of the dam, with the 100-year recurrence interval flood
3. Hydraulic (piping) failure, with the 500-year recurrence interval flood
4. Overtopping failure caused by the PMF.

In all these cases, the diversion dam would be overtopped by the floodwater released from Mackay Dam with case four being the most catastrophic. This overtopping is expected to cause the failure of the diversion dam, thus, contributing to the flooding at the INEL. The DAMBRK analysis assumes that the diversion dam begins to fail when flood waters reach 5,065 ft above msl, an overtopping depth of 0.3 ft. Because of the small size of this dam, the breach is assumed to be fully developed after 0.1 hour, an essentially instantaneous failure.

During a dam-break flood, high flows would overtop the channel banks and inundate the valley flood plain, causing significant losses of the initial flow volume. Realistic modeling of downstream flooding requires knowledge of lateral flow losses such as infiltration into the relatively-dry overbank material, depression storage losses, and side channel losses that do not return to the main flood channel.

The DAMBRK simulation routes the flood wave along the Big Lost River channel from Mackay Dam to Test Area North (TAN) at the INEL (see Figure 1-1). Outflows from the river into the Diversion Channel were estimated by the broad-crested weir outflow model included in DAMBRK.

2.3.3 Flow Rates into the INEL Diversion Area due to Hypothetical Mackay Dam Failure

PMF and overtopping failure of Mackay Dam (Scenario 4) yielded the most catastrophic results. A total of 33454.6 acre-ft of water would be diverted into Spreading Area A through the Diversion Channel, bypass swales, and other low areas to the west of the Diversion Dam from this type of dam failure. The time at which this failure scenario occurred would affect how much water was diverted. The worst case scenario would have Mackay Dam fail during a peak period of high runoff such as late June 1965 (see Figure 4-1). Figure 2-10 shows the combined inflow rates into Spreading Area A from the Mackay Dam failure and a 300% snowpack runoff.

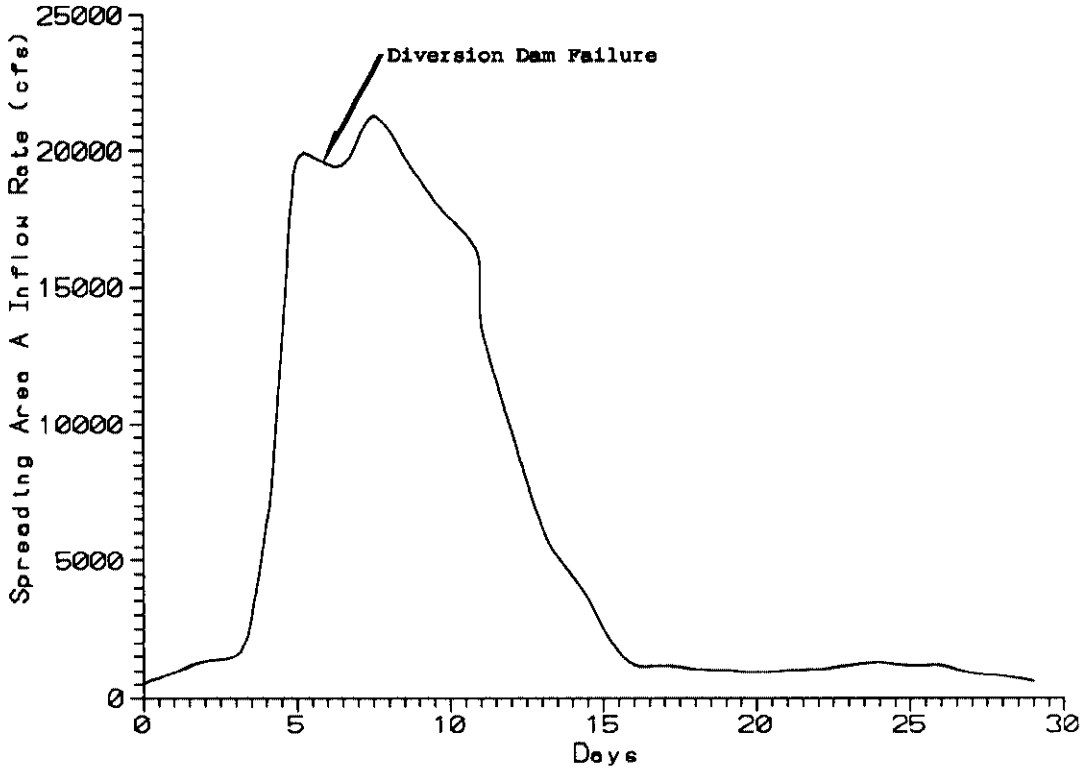

Figure 2-10 Spreading Area A inflow rates due to a Mackay Dam failure combined with a 300% snowpack runoff

Water flowing into Spreading Area A will probably increase from 2000 cfs to 20,000 cfs in a 24 hour period. Under these conditions, the Diversion Dam will probably be washed away. Even with the Diversion Dam gone, the water flowing into Spreading Area A will likely increase to a maximum rate of 22,000 cfs.

3 Dike 2 Breach Flood, Routing and Water Surface Profile Models

3.1 General modeling considerations

3.1.1 Choice of a Flood Routing Model

A first look at the uneven landscape between Dike 2 and the SDA might give the impression that a two-dimensional flow model would be required for this investigation. However, careful scrutiny of the topography would reveal that there are some fairly distinct flow paths for a breach flood from Dike 2 to the SDA. These flow paths can be modeled adequately with a one-dimensional routing model.

When choosing a one-dimensional model, the decision must be made to use either a dynamic-wave model, such as DAMBRK, or a nondynamic flow model, such as HEC-1. Several characteristics are suggested in Zovne and Wilson (1989), that favor selection of a nondynamic model. Three characteristics that fit the SDA modeling situation are as follows: (1) low head at the breach, (2) short downstream section (attenuation and timing characteristics are less important), and (3) limited engineering budget. Item 1 applies because a depth of breach of 8.6 ft maximum at Dike 2 is low compared with most dam breaches of record. Item 2 applies because the downstream section (reach) of interest, which extents to the east side of the SDA complex, is less than 2 mi long. This is a short distance for routing a flood, and the attenuation effects will be small and timing will be of little importance. Item 3 applies because developing a DAMBRK model and completing the production runs both take much more time than would be the case with an HEC-1 model. Time and budget are both limiting factors in the SDA investigation.

HEC-1 and DAMBRK have essentially the same capability for simulating a breach; the main difference between the two models is in the methods used to route the flood downstream from the breach. Although HEC-1 uses nondynamic methods for routing the flood wave, the Muskingum-Cunge routing method available in the latest version of HEC-1 produces results close to the full unsteady flow solution utilized in DAMBRK for channel slopes greater than 1 ft/mi (Brunner, 1989). The modified-Puls storage-outflow routing method used in HEC-1 also has produced results close to DAMBRK when average channel slopes are large enough so that the bed slope is the dominant term in the unsteady flow equations.

The channel slope in the SDA drainage system ranges from about 11 to 21 ft/mi in the reach which extends from the southeast corner of the SDA downstream past the security facility. The two parallel reaches immediately below the railroad embankment have slopes averaging about 50 ft/mi. With slopes this high, either the Muskingum-Cunge or the modified-Puls method in HEC-1 gives good results.

In this investigation, both the modified-Puls storage-outflow routing method and the Muskingum-Cunge routing method were used, and the results were compared. The modified-

Puls storage-outflow method is better able to account for backwater effects and storage in the flow system as compared to the Muskingum-Cunge method, but it requires the specification of the number of routing steps or subreaches to be used in the routing computation. Because the number of steps affects the attenuation of the routed hydrograph, it is an important parameter that is difficult to determine precisely in an ungauged reach. A rule of thumb for finding this value is to divide the total travel time in a reach by the computational time interval specified as input to the routing model (Hoggan, 1989). The Muskingum-Cunge method has the advantage that its solution is independent of the user-specified computational time interval.

3.1.2 Applications for a Water Surface Profile Model

The storage-outflow relationships required as input for channel routing with the modified-Puls method are developed with HEC-2 water surface profile computations. The HEC-2 model also provides discharge ratings at structures, such as the railroad embankment, and at other critical flow cross sections, such as the severe constriction near the southeast corner of the SDA. Because of the relatively small amounts of storage in the channel reaches, ratings obtained by the HEC-1 flood routing model would be less accurate than the water surface elevations computed with HEC-2.

3.2 The Modeling Approach

The modeling of the flood-flow system below Dike 2 in this investigation was accomplished in six phases:

1. A water surface profile model was developed for the entire flow system to serve the following purposes: develop storage-outflow data for routing, develop split-flow discharge ratings at the railroad embankment, develop discharge ratings at the constriction next to the southeast corner of SDA, and obtain a preliminary assessment of the hydraulics of the system.

2. An HEC-1 dam-breach and flood-routing model was developed using selected breach conditions and modified-Puls channel routing downstream from the breach. Various breach scenarios were investigated for the hypothetical release from Dike 2.

3. Because of some minor instabilities in the hydrographs generated with preliminary runs of the routing model, some of the channel reaches were modified, and two reservoirs were added. One reservoir was added upstream from the railroad embankment and the other was added next to the southwest berm of the SDA. These were modeled with modified-Puls level pool reservoir routing methods.

4. Another routing model was developed for the same flow system using

Muskingum-Cunge routing for the channel reaches. The purpose was to provide a means of verifying the results of the other model.

5. The flood-routing models developed in the previous phases were executed with selected breach parameters to determine the peak discharges at critical points in the downstream flow system.

6. HEC-2 models of the routing reaches were rerun using the peak discharges from phase five to determine final water surface elevations at key locations.

3.3 Water Surface Profile Model

3.3.1 Division of the Flow System into Routing Reaches

A water-surface profile model consisting of three major sections was developed to cover the complete flow system. It was necessary to divide the model into three sections because of the two split-flow reaches below the railroad embankment, which had to be analyzed with a graphical procedure (HEC, 1982a). HEC-2 does not have the capability to analyze bifurcated flow around an island or high ground. Thus, the model consisted of (1) an upper section extending from Dike 2 to the railroad embankment, (2) a middle section consisting of the a main-flow reach and a split-flow reach extending from the railroad embankment to a common ponding area back of the constriction near the southeast corner of the SDA, and (3) a third section extending from the constriction downstream to the lower end (see Figure 1-5).

3.3.2 Defining Model Geometry - Location of Cross Sections

A preliminary analysis of the bed slopes indicated a subcritical-flow model should be used, and the first cross section was located downstream on the drainage channel 400 ft east of the security facilities. Cross sections normal to the flow were then spaced at various intervals upstream to account for appreciable changes in cross-sectional area, roughness, or slope in the channel and overbank areas. Additional cross sections were located at the bridges and the culvert in accordance with recommended modeling procedures (HEC, 1982b). The cross sections were laid out on topographic maps of 0.5-ft and 4-ft contour intervals available at the INEL.

3.3.3 Manning's "n" Values for the Model

Because of the relatively wide, flat overbank areas along one or both sides of the drainage channel near the security facilities and at other locations upstream, effective flow areas were defined. In other words, some of the off-channel areas would store flood water;

however, because of their remoteness from the channel or peculiarities of the flow path, they would not be effective in carrying flow. To accommodate this situation in the model, these areas were assigned very high roughness coefficients (Manning's "n" values) of 0.3 to essentially block the flow.

Other typical applications of roughness coefficients used in the model are listed in Table 3-1

Table 3-1 Applications of roughness coefficients

Description	"n" value
Drainage channel bottom (gravel with weeds)	.030
Pavement (fences and other minor obstructions)	.020
Land surface (sandy with sage brush and grass)	.040
Sides of embankment (graded and short grass)	.030
Bridge opening (gravel bottom)	.030

3.3.4 Modeling Methods used at Bridges

The multiple-opening culvert and the two bridges in the existing drainage channel east of the SDA were all modeled with the normal bridge method in HEC-2. Neither of the bridges have piers, and approach roads on both sides of the bridges and the culvert are surrounded by flat areas. Because of the flatness of the surface around the bridges and culvert, overtopping of these structures would not result in well-defined weir flow. Therefore, the friction-loss solution available in the normal bridge method was the most applicable.

3.3.5 Determining Storage-Outflow Relationships for Routing

To determine storage-outflow values and discharge ratings for the routing model, several profiles were computed using a range of discharges as input. User-defined summary output tables were generated that tabulated volume and discharge for a routing reach. Travel time through the reach also was tabulated for use in determining the number of routing steps. Starting water surface elevations for these profiles were determined using normal-depth calculations.

The graphical procedure used for determining the split flow discharge rating at the railroad embankment is described in HEC, 1982a. A ridge of high ground on the downstream

side of the embankment would cause the flood flow to split; therefore, the railroad embankment, which would function as a weir, was divided into two sections at this point. Flow over both sections of the embankment were modeled with the special bridge method in HEC-2. For the section with a 2-ft box culvert, the flow was modeled as weir flow and pressure flow, and in the other section it was modeled as weir flow only.

The railroad embankment, which appears to be constructed of gravel fill material, would be eroded considerably in a dam breach flood. The modeling does not account for this eventuality because its effect on the flood peak would not be very great. The storage volume behind the railroad embankment is small, and its attenuation of the peak discharge would likewise be small. If the railroad embankment was washed out completely, the effect on the flood peak would not be significant.

3.4 Dam-Breach and Flood-Routing Model

3.4.1 Dam-Breach Simulation Characteristics

The characteristics of the hypothetical breach in Dike 2 determine the size and shape of the flood hydrograph that is routed through the drainage system. In HEC-1, the breach is initiated when the water surface in the reservoir reaches a given elevation. The breach begins at the top of the dam and expands linearly to the bottom elevation of the breach and to its full width in a given time. The outflow is computed as trapezoidal broad-crested weir flow. The parameters required for input to the program include (a) the top-of-dam elevation, (b) the water surface elevation at which the failure begins, (c) the elevation of the bottom of the breach when it is fully formed, (d) the full width of the bottom of the breach, (e) the side slopes of the breach, and (f) the duration of time required for the breach to develop. Triangular, rectangular, or trapezoidal breach shapes can be simulated by specifying different combinations of bottom-width and side-slope values.

Because, breach characteristics are related to structural characteristics of the dam (e.g., height, width, and the material with which the dam is constructed), past dam failures have been analyzed to develope criteria for setting breach parameters. A number of Government agencies have adopted such criteria. Some of the studies that have been done and the criteria that have been developed were reviewed and compared to determine their applicability to the Dike 2 breach simulation.

3.4.2 Potential Breach Conditions at Dike 2

Of the causes of failure that have been identified, internal erosion (seepage failures) of the embankment or its foundation is most applicable to Dike 2. Uncontrolled seepage can cause soil erosion within an embankment or its foundation, which may result in piping failure or structural collapse. Piping can occur when strata of high permeability, cavities, or fissures

permit direct flow of water from the reservoir. Leakage from reservoirs with pervious dam foundations sometimes causes piping. This is most common where there are traces of sand or gravel within the deposits on which the dam has been built. However, the open joints in basalt, sandstones, and other rocks can also give rise to seepage paths.

> Piping is progressive internal soil erosion. It begins at a point of concentrated seepage where the hydraulic pressure gradients are sufficiently high to produce eroding velocities. If the point of soil erosion is on the face of the dam or some other location where the eroded soil can be carried away a small cavity is produced. This causes an increased concentration of seepage, more erosion and an elongation of the cavity towards the source of the seepage. The further the cavity or pipe extends upstream, the shorter the seepage path becomes. The gradients increase and the erosion becomes faster until the cavity suddenly breaks through the remaining soil into the reservoir. The rush of water through the completed pipe can rapidly increase the diameter of the opening from perhaps only a few millimeters to several meters and can result in the structural collapse of the dam and the formation of a breach. Thereafter the failure process becomes similar to that of overtopping. (Binnie & Partners, 1986)

Although seepage failures may be the most plausible for a failure at Dike 2, the possibility of occurrence is rather remote because the parameter most related to this condition is dam height. There is evidence from the Binnie & Partners study of dam failures in England that higher dams are more likely to experience seepage problems. Over 50 percent of such failures studied occurred on dams of 20 m or more in height.

Other causes of dam failure in the literature that appear less applicable to Dike 2 conditions are not described here. However, earth and rockfill embankments stand up well to earthquake loads and shaking. Failures that have occurred have usually been associated with smaller dams built of sand and silty materials, particularly those constructed with hydraulic fill.

3.4.3 Criteria for Selecting Breach Parameters

Several criteria taken from the literature for setting breach parameters are summarized as follows:

Study of 11 dam failures in the United States and United Kingdom (Hughes, 1981)

Breach width = 3.75 height of dam

Study of dam failures in the UK (Binnie & Partners, 1986)

> Clearly, the preponderance of UK cases have Bw/H values in the range 1 to 3 with those for the two piping failures both less than 2. ...the breach height is effectively the height of the dam.

Guidelines for evaluation of hydropower projects (Office of Power Licensing, 1987).

> Average width of breach (earthen, rockfill, timber crib) "usually between 2HD and 4HD" HD = Height of dam Horizontal component "Z" of side slope of breach (all):
>
> $0 \leq Z \leq 2$
>
> Time to failure "TFH" in hours (all):
>
> $0.1 \leq TFH \leq 1$

Bureau of Reclamation dam safety procedures (Bureau Reclamation, 1989)

> For earthfill dams:
> Breach width (average) 1/2 to 3 times the dam height
> Side slope of breach 0.1 to 1:1
> Failure time (hours) 0.5 to 4

National Research Council dam safety guidelines (Committee on the Safety of Existing Dams, 1983)

> The maximum width of breach may be estimated by dividing the area of the dam (measured along the axis) by the maximum height of the dam

"Breaching Characteristics of Dam Failures" (MacDonald and Langridge-Monopolis, 1984)

> Breach development parameters are taken from graphs based on the volume of breach material removed during breach formation and a breach formation factor (BFF). The most common side slopes were found to be 2V:1H.

3.4.4 Application of Breach Criteria to Dike 2

These criteria are not entirely consistent and do not apply precisely to Dike 2 conditions. They were developed from a wide range of dams, many with characteristics quite different than Dike 2. Because an in-depth analysis of breach conditions is beyond the scope of this investigation, two sets of parameters were selected that bracket the conditions at Dike

2; these parameters were developed from historical breach events.

A breach-width criterion of 2 times the dam height fits within several of the recommendations made in the literature, so this was selected for determining one of the values for this parameter. This gives a breach width of 17 ft. The largest breach-width parameters were determined with the criteria proposed by MacDonald and Langridge-Monopolis (1984). According to this criteria for nonearthfill dams, which includes rockfill embankments, the breach width for Dike 2 would be about 640 ft wide.

This extreme width resulted from applying values for the large volume of storage behind Dike 2 and the relatively small embankment height to the criteria in this reference. The criteria suggested by the Committee on the Safety of Existing Dams (1983) also indicate an extremely wide breach. Because of the great divergence in results between these criteria and the results of other criteria reviewed and the fact that these criteria appeared unapplicable because of length-height conditions of the dike, they were not used. The criterion (BW = 3.75 H) suggested in Hughes (1981) was selected for determining the upper end values; it gave a breach width of 31 ft.

For the other breach parameters, side slopes ranging from 0.1H:1V to 2H:1V, and breach-failure times of 0.1 to 4 hours were selected and analyzed.

3.4.5 Flood routing model

A schematic of the flood routing model as finally developed is shown in Figure 3-1. The routing reaches are indicated with arrows.

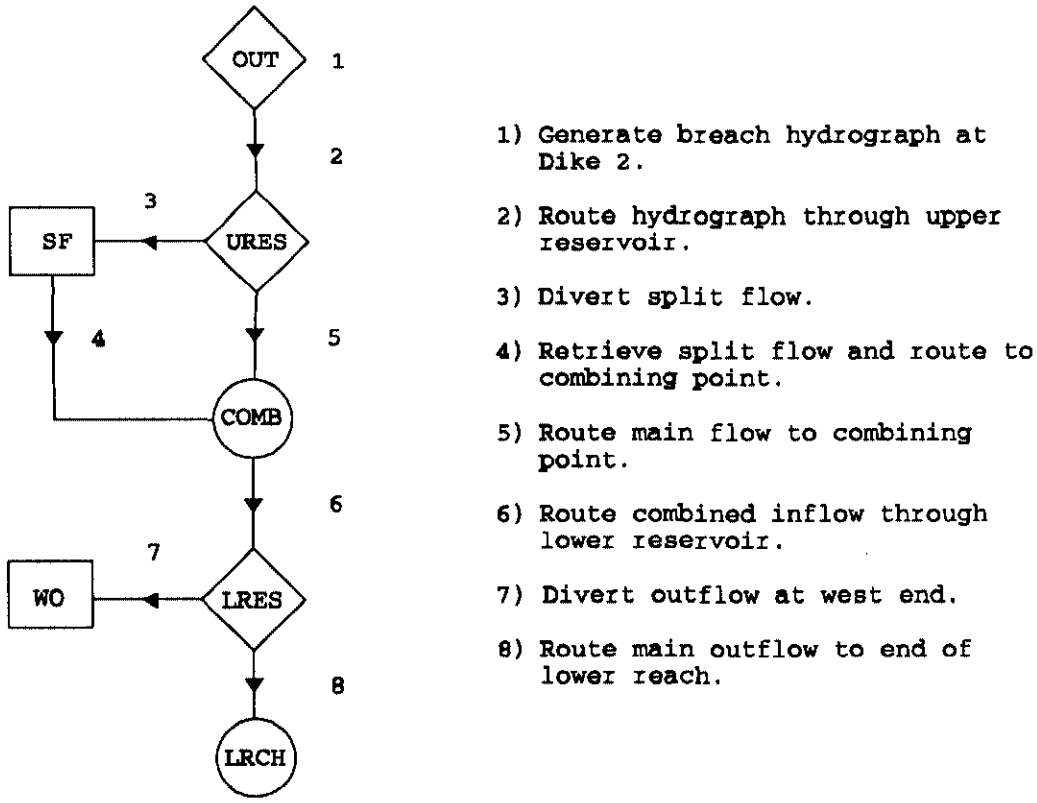

Figure 3-1 Schematic of HEC-1 flood-routing model

The flood hydrograph to be routed through the system is generated by simulating a breach opening and allowing the volume of water impounded in spreading Area B at its maximum level to flow out. The fact that inflow to Spreading Area B will be occurring from an extreme event at the same time the breach occurs will be insignificant to the outflow hydrograph. The reservoir water level near its peak varies by only 0.02 ft in 10 hours. The peak flow generated by the breach will be fully developed and routed past the SDA in much less than 10 hours.

Because the HEC-1 program requires an inflow hydrograph to the reservoir to initiate a dam-breach computation, an insignificant inflow hydrograph is entered in input.

As the schematic indicates, the flood from Spreading Area B is first routed to the railroad embankment through the upper small detention basin. At this point a diversion is made based on the split-flow rating developed previously with the HEC-2 model. The main flow and the split flow are both routed downstream, though in different paths, to the detention basin on the southwest side of the SDA. The two flows are combined and routed through the detention basin to outlets at both ends of the basin. The storage-outflow relationship for the reservoir routing accounts for discharge from both the west end and the east end. To adjust the flow for routing downstream past the east side of the SDA to the lower end of the study

reach, the equivalent of the outflow from the west end is diverted from the total outflow from the reservoir.

3.4.6 Routing Model Revised to Incorporate Muskingum-Cunge Routing Method

Because the Muskingum-Cunge method produces results comparable to a dynamic wave model in reaches with adequate slope, a version of the routing model using this method was created. Results from this model were used for comparison with and verification of the other model. The Muskingum-Cunge channel routing technique is a nonlinear coefficient method that accounts for hydrograph diffusion based on physical channel properties and the inflow hydrograph. HEC-1 input developed for each routing reach includes a representative channel cross section, reach length, Manning's roughness coefficients, and channel bed slope.

4 Results and Conclusions

4.1 INEL Diversion Area Flow System Model Results

4.1.1 Model Calibration

Before simulating the hypothetical Mackay Dam failure effects on the Diversion Area, the INEL Diversion Area Flow System Model must be calibrated. Calibration is the process where the model's physical parameters are adjusted so that a simulation will yield results comparable to the results observed from a known event. In this case, the known event is the 1965 flood. This event was chosen because the data collected in Barraclough et al., 1967, is the most complete covering a period of time when water was flowing into and ponding in the Diversion Area.

Between October 1964 and September 1965, almost 400,000 acre-ft of water passed by the gauging station below Mackay Reservoir (Barraclough et al., 1967). For the period of April through December 1965, 119,000 acre-ft of water flowed past the gauging station below the Diversion Dam, and 115,000 acre-ft flowed into the Diversion Area. On June 8, part of the Big Lost River discharge was diverted into the Diversion Area and nearly filled spreading areas A, B, and C by mid-July. Flow into the Diversion Area stopped on July 30, and by mid-August, the ponds were dry. Later in August, water was again flowing into the Diversion Area. The flow lasted until the end of 1965. Figure 4-1 is a hydograph of the volumetric diversion flow that occurred from June 8, 1965 to July 30, 1965.

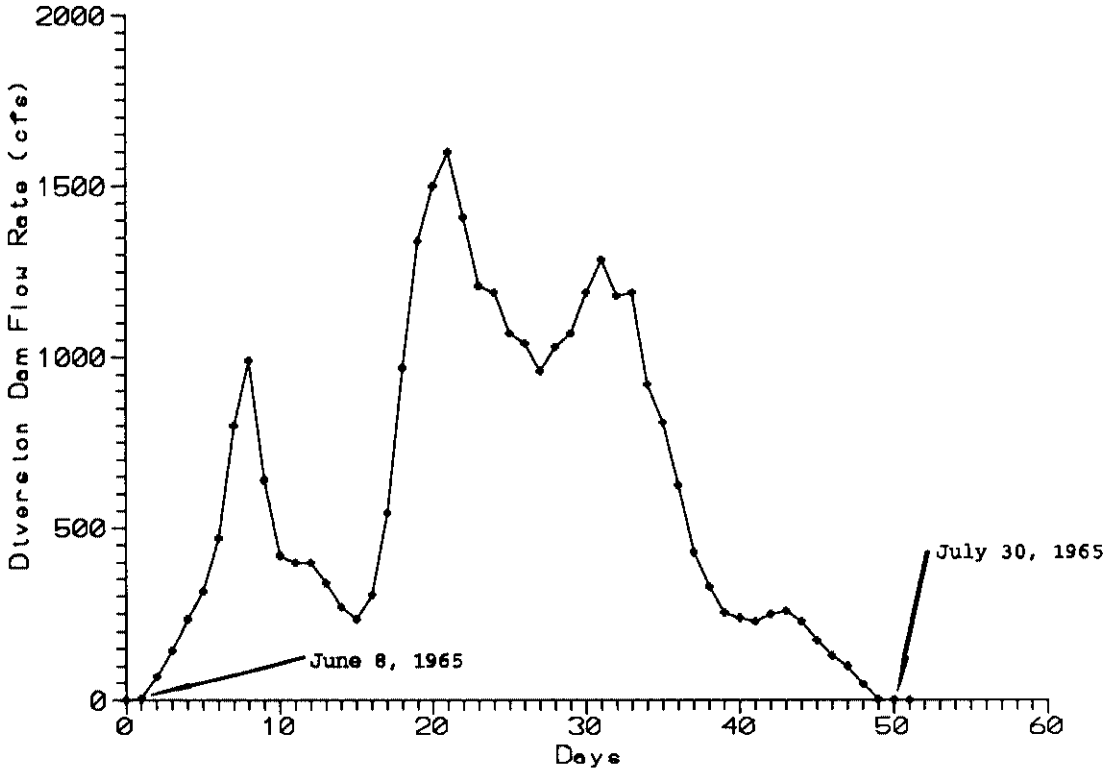

Figure 4-1 Hydrograph of volumetric flow in the diversion channel from June 8, 1965 to July 30, 1965

On June 29, 1965, a peak flow in the diversion channel was measured to be 1800 ft^3/s (Barraclough et al., 1967) with an average of 1600 ft^3/s for the day. That same day, the highest recorded water surface elevation in Spreading Area A was 5043.7 ft above msl. Storage in Area A for this elevation was 2300 acre-ft. This storage value is very close to the 2270 acre-ft interpolated from Table 2-1. Also on June 29, the highest recorded water surface elevation in Spreading Area B was 5037.7 ft above msl. A discussion with Barraclough indicated that this value of elevation is not necessarily the absolute peak value because he was not able to measure the water surface elevations daily. Model simulations show that peak water surface elevation in Spreading Area B lags peak elevation in Spreading Area A by 1 to 2 days because of the constricted flow in the connecting channel. The lag time varies due to the difference in magnitudes of the diverted flow between different simulations.

It is doubtful that water surface elevations and channel flows would occur the same today (1990) as it did in 1965 because of the many physical modifications that have been made to the Diversion Area since 1965. The wide shallow depressions that connect Spreading Areas B, C, and D have been bulldozed to clear brush and lower the elevation at which water would flow into areas C and D. The connecting and diversion channels have been modified to increase flow capacity. Also, the storage capacities of the spreading areas

have been increased by adding 8 ft in elevation to Dikes 1 and 2. In 1965, Spreading Areas A, B, and C contained ponded water while Spreading Area D did not. Today, given the same Big Lost River discharge of 1965, Spreading Areas A through D would probably have some water ponded in them. Having the water spread over a larger surface area would result in lower water surface elevation in Spreading Area B. Spreading Area A would probably have a lower water surface elevation because flow out of the area would occur at a greater rate because of the increased connecting channel flow.

Calibration of the INEL Diversion Area Flow System Model is based upon the 1965 diversion flow rates and the assumption that Spreading Area D will also be flooded. The model assumes that Spreading Areas B through D simulate a single reservoir because the flow paths interconnecting Spreading Areas B, C, and D are not well defined. The model then assumes water infiltrates in Spreading Areas B through D as soon as water begins flowing in the connecting channel. In actuality, the water level in Spreading Area B must reach a certain level before water flows into Spreading Areas C and D. Therefore, volumetric infiltration in the model initially occurs at a faster rate than would occur in the Diversion Area. To compensate for this, the model infiltration rates for the individual spreading areas are lower than the actual infiltration rates measured by Barraclough.

The model infiltration rates are 0.3 ft/d for Spreading Area A and 1.1 ft/d for Spreading Areas B through D and the Offsite Spreading Area. With these values, the model simulation for June 29, 1965, taking into account the present Diversion Area flow characteristics, yielded a Spreading Area A water surface elevation of 5043.7 ft above msl. This is the same water level as the measured 1965 value even though the model infiltration rate is 0.3 ft/d versus the measured value of 0.71 ft/d. This is due to the model employing a connecting channel with an increased flow capacity. The simulation predicts that peak water surface elevation in Spreading Area B will be 5036.7 ft above msl. This is 1 ft lower than the actual measured value from 1965 even though the model infiltration rate is 1.1 ft/d versus the measured 2.6 ft/d value. This is due to the model assuming flow into Spreading Area D at all times the connecting channel has flow. In an actual event, water will flow into Spreading Area D only when the water level in Spreading Area B is sufficient. This flow into area D will still keep the water level in Area B lower than it was in 1965. The model simulation also predicts that the water surface elevation in Spreading Area D would be lower than the Dike 3 weir.

4.1.2 Model Results for the Hypothetical Mackay Dam Failure

The model simulation time of the INEL Diversion Area during a hypothetical Mackay is 50 days (1200 hours) and coincides with the 1965 flood hydrograph. A Mackay Dam failure is considered to be the practical limit of water available to discharge in the Big Lost River Drainage Basin. To simulate maximum inflow into Spreading Area A, the peak flow at the INEL Diversion Dam due to a Mackay Dam failure coincides with the peak flow recorded in the 1965 flood. The hydrograph into Spreading Area A resulting from this theoretical peak

river discharge is illustrated in Figure 2-10. The model results for the water surface elevations in the spreading areas is shown in Figure 4-2

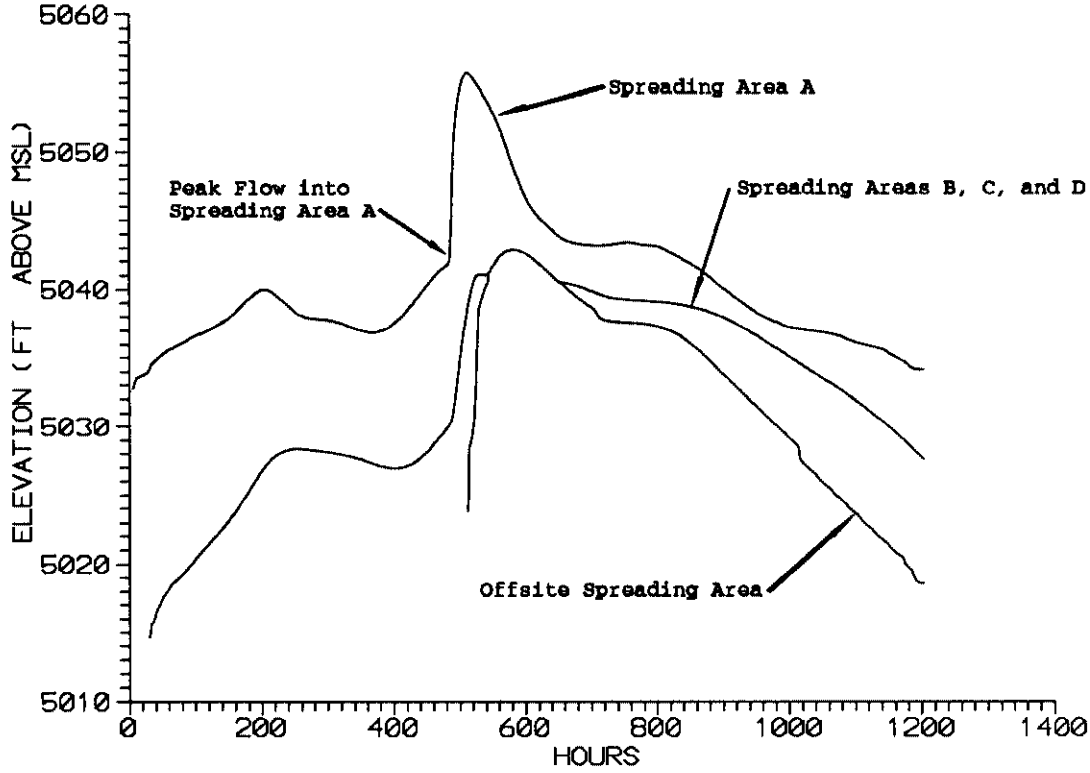

Figure 4-2 Water surface elevations compared to simulation time for the Diversion Area in the case of the hypothetical Mackay Dam failure

The model predicts that at 508 hours into the simulation, the water surface elevation in Spreading Area A reaches a maximum of 5055.92 ft above msl. The water surface elevation in Spreading Areas B, C, and D is 5037.31 ft above msl, which is the elevation that water just begins to flow through the Dike 3 Weir into the Offsite Spreading Area. At this point in time, Spreading Area A contains approximately 23,600 acre-ft of water and Spreading Areas B, C, and D contain a total of 16,500 acre-ft of water.

Previous calculations (Bennett, 1986) predict that when the diversion channel is running at peak discharge (7200 ft^3/s), Dike 1 near the diversion dam begins to be overtopped when the water surface elevation in Spreading Area A reaches an elevation of 5054.8 ft above msl. This is due to the backwater effect in the diversion channel. With a maximum predicted water surface elevation of 5055.92 ft above msl, not only will the Diversion Dam fail but a large portion of Dike 1 forming the diversion channel will probably erode away. The model does not take into account the possible failure of a portion of Dike 1. If a portion of Dike 1 fails, the peak water surface elevations in the spreading areas will probably be less.

At 577 hours into the simulation, the peak water surface elevation of 5043.02 ft above msl is reached in Spreading Areas B, C, and D and the Offsite Spreading Area. This water surface elevation is still 9.98 ft below the top of Dike 2 (5053 ft above msl) but is 2.4 ft over the top of Dike 3 (5040.6 ft above msl). The combined storage of Spreading Areas B, C, and D is approximately 25,400 acre-ft of water. The Offsite Spreading Area contains approximately 5,840 acre-ft of water at 5043.02 ft above msl. At this point in time, the water surface elevation of Spreading Area A is 5049.25 ft above msl. Spreading Area A will contain approximately 5730 acre-ft of water. The total storage in the Diversion Area is approximately 37,000 acre-ft of water.

Dike 3 would fail or seriously erode if the water level overtops the dike, but this is not addressed in the model. The model assumes that when the water surface elevation of the Offsite Spreading Area rises above the top of Dike 3 by overtopping (the Offsite Spreading Area cannot fill completely by Dike 3 Weir flow alone), Spreading Areas B, C, and D, and the Offsite Spreading Area act as one pond. Referring to Figure 4-2, the water surface elevations in Spreading Areas B, C, and D, and the Offsite Spreading Area coincide between simulation hours 541 and 647. After hour 647 there is a separation in the water surface elevations of Spreading Areas B, C, and D and the Offsite Spreading Area. This is primarily due to the larger flow rate of the connecting channel into Spreading Area B then the Dike 3 flow into the Offsite Spreading Area.

4.1.3 Conclusions

The INEL Diversion Area Flow System Model has been calibrated from a conservative point of view. Conservative in this case refers to higher peak water surface elevations in the spreading areas than would realistically occur in an actual event of a large Big Lost River discharge. The conservative nature of the model is due to the use of lower than measured infiltration rates and the assumption that no failure of the dike system would occur. The model was designed to predict the upper limit that the peak water surface elevations of the spreading areas would reach, and more importantly, the highest possible water surface elevation that Dike 2 would encounter.

In an actual event, such as in the hypothetical Mackay Dam failure scenario, it is likely that the peak water surface elevation in Spreading Area B would not reach 5043.02 ft above msl. If a portion of Dike 1 along the connecting channel fails, much of the water in the channel would not flow into the Diversion Area. It may then be possible that an insufficient amount of water will end up in Spreading Area D to overtop Dike 3. If this were the case, the water surface elevation next to Dike 2 would be less than 5040.6 ft above msl.

4.2 Peak Discharges and Water Surface Levels at the SDA

4.2.1 Results of Model Computations

Breach parameters, selected to bracket the range of breach conditions reported in the literature, excluding the two that were considered non applicable, were applied to the flood routing and water surface profile models developed for this investigation and are shown in Table 4-1.

Table 4-1 Breach parameters

	Low	High
Maximum WS elevation behind dike (ft)	5043.0	5043.0
Breach bottom elevation (ft)	5034.7	5034.7
Breach bottom width (ft)	17	31
Breach side slopes	1:1	1:1
Breach-failure time (hr)	1	1

A sensitivity analysis of failure times from 0.1 to 4 hours indicated that within the range of values suggested in the literature, this parameter has insignificant effect on the peak discharge produced by the breach. Another comparative analysis of side slopes (H:V) from 0.1 to 2 revealed that this parameter can make a substantial difference in the peak discharge. A slope of 1:1 was selected because it fits the conditions of the rock fill at Dike 2. These two sets of conditions defined by the low and high criteria produced the following peak discharges at the breach: low = 1733 ft^3/s and high = 2759 ft^3/s.

Results in routing the breach hydrograph downstream with the model incorporating the Muskingum-Cunge (M-C) channel routing method compared almost identically with the results of the model using modified-Puls (M-P) channel routing. The peak discharges produced by the two models for the other flows at key locations appear in Table 4-2.

Table 4-2 Peak discharges at key locations

Location		Peak Discharges (ft^3/s) M-C	M-P
Flow over the railroad embankment	Low	1712	1712
	High	2728	2728
Inflow to detention basin southeast side of SDA from split-flow reach	Low	411	414
	High	797	887
Inflow to detention basin southeast side of SDA from main-flow reach	Low	1301	1302
	High	1930	1932
Outflow from detention basin at constriction near the southeast corner of SDA	Low	1573	1573
	High	2115	2115
Lower end of study reach at east of security facility	Low	1573	1567
	High	2114	2111
Outflow around southwest corner of the SDA	Low	97	97
	High	507	507

Final water-surface elevations next to the SDA, computed with HEC-2 based on the final peak discharges computed in the lower reach, appear in Table 4-3

Table 4-3 Final water-surface elevations next to SDA

Location		Peak Discharge (ft^3/s)	W S Elevation (ft)
Constriction near southeast corner of SDA (detention basin outlet - cross section 24)	Low	1567	5011.29
	High	2111	5013.84
Constriction between SDA and TSA about 300 ft north of SDA southeast corner (cross section 19)	Low	1567	5011.29
	High	2111	5011.89
Drainage channel about 400 ft southeast of security facility (cross section 4)	Low	1567	5007.78
	High	2111	5008.14

4.2.2 Conclusions

This investigation has shown that the SDA berm is not in danger of being overtopped by a breach flood except under the most extreme case investigated (high criteria). In this case, the water-level elevation of 5014.36 ft above msl in the lower detention basin would overtop the SDA berm at the southwest access-road crossing and for a distance of 500 ft next to the constriction near the southeast corner.

At this reservoir level (5014.36 ft above msl) there would also be a small outflow around the west end of the SDA. This flow would cross over the saddle in the west access road and into the low areas on the north side. There is a possibility of a small amount of flow overtopping the SDA berm at the west access-road crossing if this should occur.

Along the northeast berm next to the TSA, especially near the southeast corner, the water surface elevations are close to or slightly above the top. There also would be some flow through the TSA on the east side of the barrel storage pad and on the east side of the covered storage facility.

The existing drainage channel east of the SDA is not sufficient to carry floods generated under either low or high breach criteria without overtopping its banks. Under either set of parameters, the flow would be out of the banks, and there would be several inches of water over the pavement near the security facility and other buildings along Adams Boulevard.

The breach size modeled under the high criteria is in reality too high for the

conditions at Dike 2. The breach width for this case was computed from the maximum depth of the embankment (8.3 ft) with the relationship (BW = 3.75 H). This relationship produces greater widths than have actually occurred in many of the breaches that have been studied. As reported in the study of dam failures by Binnie & Partners (1986), "the preponderance of UK cases have BW/H values in the range of 1 to 3 with those for the two piping failures both less than 2." Based on this, it could be assumed that the low breach criteria is more applicable and that the SDA berm would not be overtopped.

Because there would be a very large volume of water stored behind Dike 2 at the maximum water level elevation of 5043.0 ft above msl, there would be considerable exposure of the breach to erosive action of the outflow. According to the criteria developed by MacDonald and Langridge-Monopolis (1984) this would result in a very wide breach in a very short time. This wide breach would result in a very high peak discharge that would cause considerable flooding at the SDA.

However, if a wide breach was eroded by the large volume of water flowing through the breach, the large rock composition of the riprap embankment (very large rocks) would show that the development of the breach to a relatively long duration of time. In which case, the peak discharge would be relatively small.

REFERENCES

Atomic Energy Commission - Idaho Operations Office, Division of Engineering and Construction, Idaho Falls, Idaho, Contract AT(10-1)-12, 1949

J. T. Barraclough, W. E. Teasdale, and R. G. Jensen, Hydrology of the National Reactor Testing Station, Idaho, 1965, USGS, 1967.

C. M. Bennett, Capacity of the Diversion Channel below the Flood - Control Dam on the Big Lost River at the Idaho National Engineering Laboratory, Idaho, USGS, 1986.

Binnie & Partners, Consulting Engineers, Modes of Dam Failure and Flooding Damage Following Dam Failure, Final Report to the Department of the Environment (Contract No. PECD 7/7/184), 1986.

Gary W. Brunner, Muskingum-Cunge Channel Routing, Lecture L1277, Hydrologic Engineering Center, U.S. Army Corps of Engineers, Davis, Calif., 1989.

Bureau of Reclamation, Policy and Procedures for Dam Safety Modification Decision Making, U.S. Department of the Interior, Denver, Colorado, April 1989.

M. Hanif Chaudhry, Ph.D., Applied Hydraulic Transients, Van Nostrand Reinhold Co., 1979.

Committee on the Safety of Existing Dams, Safety of Existing Dams: Evaluation and Improvement, National Research Council, National Academy Press, Washington, D.C., 1983.

George Fleming, Computer Simulation Techniques in Hydrology, Elsevier, 1975.

Daniel H. Hoggan, Computer-Assisted Floodplain Hydrology and Hydraulics, McGraw-Hill, New York, 1989.

A. K. Hughes, The Erosion Resistance of Compacted Clay Fill in Relation to Embankment Overtopping, Ph.D. Thesis, University of Newcastle-upon-Tyne, Newcastle, England, 1981.

Hydrologic Engineering Center, HEC-1 Flood Hydrograph Package, Users Manual, U.S. Army Corps of Engineers, Davis, Calif., 1981 (rev. 1987).

Hydrologic Engineering Center, HEC-2 Water Surface Profiles, Users Manual, U.S. Army Corps of Engineers, Davis, Calif. 1982.

Hydrologic Engineering Center, Application of HEC-2 Split Flow Option, Training Document No. 18, U.S. Army Corps of Engineers, Davis, Calif., April 1982.

ISCO, Open Channel Flow Measurement Handbook, ISCO, Ic., 1981

K. N. Koslow and D. H. Van Haaften, Flood Routing Analysis for a Failure of Makay Dam, EG&G Idaho, Inc., 1986.

R. D. Lamke, Stage - Discharge Relations on the Big Lost River within National Reactor Testing Station, Idaho, USGS, 1969.

Ray K. Linsley and Joseph B. Franzini, Water - Resources Engineering, McGraw - Hill, 1979.

Thomas C. MacDonald, and Jennifer Langridge-Monopolis, "Breaching Characteristics of Dam Failures," Journal of Hydraulic Engineering, ASCE, vol. 110, no. 5, May 1984.

J. D. McKinney, Big Lost River 1983 - 1984 Flood Threat, EG&G Idaho, Inc., 1985.

Office of Power Licensing, Engineering Guidelines for the Evaluation of Hydropower Projects, Federal Energy Regulatory Commission, July 1987.

Roberson and Crowe, Engineering Fluid Mechanics, 3rd Ed.,Houghton Mifflin Co., 1985

J. B. Robertson, Robert Schoen, and J. T. Barraclough, The Influence of Liquid Waste Disposal on the Geochemistry of Water at the National Reactor Testing Station, Idaho: 1952 - 1970, USGS, 1974.

USGS, Big Southern Butte, Idaho, 1972.

Viessman, Knopp, Lewis, and Harbough, Introduction to Hydrology, Harper and Row, 1977.

E. M. Wilson, Engineering Hydrology, Halsted Press, 1974.

Jerry Zovne, and Stuart R. Wilson, "Dynamic Versus Non-Dynamic Modeling of Dam Safety Related Breach Analyses," Association of State Dam Safety Officials, Newsletter, vol. 5, no. 4, Nov., 1989.

APPENDIX

```
      PROGRAM DAFLOW
C PROGRAM DAFLOW ESTIMATES SURFACE WATER LEVELS IN THE DIVERSION AREA AT
C INEL BASED UPON THE CONTINUITY OF MASS STORAGE COMPARED TO STORAGE
C VALUES DEVELOPED FROM DIGITIZED CONTOUR MAPS.  ALL ELEVATIONS ARE
C IN NRTS DATUM
C NMAX => MAXIMUM NUMBER OF VALUES IN A DATA TABLE
      IMPLICIT REAL*8(A-H,O-Z)
      PARAMETER (NMAX=200)
      COMMON/FLAGS/ISSFLG,IRAIN,IFLOW
      COMMON/NTABS/NATB,NBCDTB,NOSTB,NVFTB,NRNTB
      DIMENSION ATAB(NMAX,3),BCDTAB(NMAX,3),OSTAB(NMAX,3)
      DIMENSION VFTAB(NMAX,2),RNTAB(NMAX,2)
C
      CALL INPUT(NMAX,ZA,ZB,S,B,THET,XKIA,XKIB,XKE,XN,DT,ST,ET,NPRNT,
     +ATAB,BCDTAB,OSTAB,CFLOW,CRAIN,VFTAB,RNTAB)
      CALL DRAIN(NMAX,ZA,ZB,S,B,THET,XKIA,XKIB,XKE,XN,DT,NPRNT,ST,ET,
     +ATAB,BCDTAB,OSTAB,CFLOW,CRAIN,VFTAB,RNTAB)
      STOP
      END
C
      SUBROUTINE INPUT(NMAX,ZA,ZB,S,B,THET,XKIA,XKIB,XKE,XN,DT,ST,ET,
     +NPRNT,ATAB,BCDTAB,OSTAB,CFLOW,CRAIN,VFTAB,RNTAB)
C THIS SUBROUTINE INPUTS ALL FLOW PARAMETERS.
C
C ISSFLG => STEADY-STATE OR VARIABLE FLOW FLAG
C        ISSFLG = 0 STEADY-STATE FLOW PROBLEM
C                 IRAIN = -1 OR 0
C        ISSFLG = 1 VARIABLE FLOW PROBLEM
C                 IRAIN = -1 OR 0 OR 1
C IRAIN => PRECIPITATION CONTROL FLAG
C       IRAIN = -1 NO PRECIPITATION
C       IRAIN =  0 CONSTANT PRECIPITATION
C       IRAIN =  1 VARIABLE PRECIPITATION
C ZA => ELEVATION OF INLET TO Connecting Channel
C ZB => ELEVATION OF OUTLET OF Connecting Channel
C XL => LENGTH BETWEEN INLET AND OUTLET OF Connecting Channel
C S => SLOPE OF Connecting Channel
C B => HYDRAULIC EQUIVALENT OF CHANNEL BASE WIDTH
C THET => ANGLE OF CHANNEL WALL DEPARTURE FROM THE NORMAL TO THE CHANNEL
C XKIA => INFILTRATION RATE PER UNIT AREA IN SPREADING AREA A
C XKIB => INFILTRATION RATE PER UNIT AREA IN SPREADING AREAS B,C,D, AND
C         OFFSITE
C XKE => EVAPORATION RATE PER UNIT AREA
C XN => ROUGHNESS COEFFICIENT OF CHANNEL
C DT => TIME STEP LENGTH
C ST => START TIME
C ET => STOP TIME
C NPRNT = > PRINT INTERVAL. NUMBER OF TIME STEPS BETWEEN PRINTS
C ATAB => TABLE ARRAY HOLDING AREA AND VOLUME VALUES Vs. YA
C     ATAB(I,1) = ELEVATION OF THE WATER SURFACE FOR AREA A, YA
C     ATAB(I,2) = AREA OF SPREADING AREA A AT YA
C     ATAB(I,3) = VOLUME OF SPREADING AREA A AT YA
C BCDTAB => TABLE ARRAY HOLDING AREA AND VOLUME VALUES Vs. YB
C     BCDTAB(I,1) = ELEVATION OF THE WATER SURFACE FOR AREAS BCD, YB
C     BCDTAB(I,2) = AREA OF SPREADING AREA BCD AT YB
C     BCDTAB(I,3) = VOLUME OF SPREADING AREA BCD AT YB
C OSTAB => TABLE ARRAY HOLDING AREA AND VOLUME VALUES Vs. YA
C     OSTAB(I,1) = ELEVATION OF THE WATER SURFACE FOR OFFSITE AREA AT YB
C     OSTAB(I,2) = AREA OF OFFSITE SPREADING AREA AT YB
C     OSTAB(I,3) = VOLUME OF OFFSITE SPREADING AREA AT YB
C CFLOW => CONSTANT VALUE OF VOLUMETRIC INFLOW FOR THE DIVERSION CHANNEL
C          ONLY REQUIRED WHEN ISSFLG = 0
C VFTAB => TABLE ARRAY HOLDING VOLUMETRIC INFLOW RATES FOR THE DIVERSION
C          CHANNEL Vs. TIME. ONLY REQUIRED WHEN ISSFLG = 1
C     VFTAB(I,1) = TIME /DAYS
C     VFTAB(I,2) = VOLUMETRIC INFLOW RATES
C CRAIN => CONSTANT VALUE OF VOLUMETRIC INFLOW PER UNIT AREA FOR
C          THE TOTAL DIVERSION AREA. ONLY REQUIRED WHEN IRAIN = 0
C RNTAB => TABLE ARRAY HOLDING VOLUMETRIC INFLOW RATES PER UNIT AREA FOR
C          THE TOTAL DIVERSION AREA. ONLY REQUIRED WHEN IRAIN = 1
C     RNTAB(I,1) = TIME
C     RNTAB(I,2) = VOLUMETRIC INFLOW RATES PER UNIT AREA
C NATB => NUMBER OF DATA POINTS IN ATAB
C NBCDTB => NUMBER OF DATA POINTS IN BCDTAB
```

```
C NOSTB => NUMBER OF DATA POINTS IN OSTAB
C NVFTB => NUMBER OF DATA POINTS IN VFTAB
C NRNTB => NUMBER OF DATA POINTS IN RNTAB
      IMPLICIT REAL*8(A-H,O-Z)
      COMMON/FLAGS/ISSFLG,IRAIN,IFLOW
      COMMON/NTABS/NATB,NBCDTB,NOSTB,NVFTB,NRNTB
      CHARACTER IN*20,OUT*20
      DIMENSION ATAB(NMAX,3),BCDTAB(NMAX,3),OSTAB(NMAX,3)
      DIMENSION VFTAB(NMAX,2),RNTAB(NMAX,2)
C
      WRITE(*,*)' ENTER FILE NAME  '
      READ(*,*)IN
      OPEN(UNIT=9,FILE=IN,STATUS='OLD')
C
      WRITE(*,*)' ENTER OUTPUT FILE NAME  '
      READ(*,*)OUT
      OPEN(UNIT=19,FILE=OUT)
C
      READ(9,*)ISSFLG,IRAIN
C
      IF(ISSFLG.EQ.1)THEN
      WRITE(*,20)
      WRITE(19,20)
   20 FORMAT(/' FLOW INTO SPREADING AREA A IS VARIABLE')
      IF (IRAIN.EQ.-1)WRITE(*,21)
      IF (IRAIN.EQ.-1)WRITE(19,21)
   21 FORMAT(' NO PRECIPITATION ')
      IF (IRAIN.EQ.0)WRITE(*,22)
      IF (IRAIN.EQ.0)WRITE(19,22)
   22 FORMAT(' CONSTANT PRECIPITATION ')
      IF (IRAIN.EQ.1)WRITE(*,23)
      IF (IRAIN.EQ.1)WRITE(19,23)
   23 FORMAT(' VARIABLE PRECIPITATION ')
      ENDIF
C
      IF(ISSFLG.EQ.0)THEN
      WRITE(*,24)
      WRITE(19,24)
   24 FORMAT(/' FLOW INTO SPREADING AREA A IS CONSTANT')
      IF (IRAIN.EQ.-1)WRITE(*,25)
      IF (IRAIN.EQ.-1)WRITE(19,25)
   25 FORMAT(' NO PRECIPITATION ')
      IF (IRAIN.EQ.0)WRITE(*,26)
      IF (IRAIN.EQ.0)WRITE(19,26)
   26 FORMAT(' CONSTANT PRECIPITATION ')
      ENDIF
C
      READ(9,*)ZA,ZB,XL
      S = DABS(ZA-ZB)/XL
      WRITE(*,27)ZA,ZB
      WRITE(19,27)ZA,ZB
   27 FORMAT(/' ELEVATION OF CONNECTING CHANNEL INLET = ',1PE11.4,' Ft.'/
     +' ELEVATION OF CONNECTING CHANNEL OUTLET = ',1PE11.4,' Ft.')
      WRITE(*,28)XL,S
      WRITE(19,28)XL,S
   28 FORMAT(' LENGTH BETWEEN INLET AND OUTLET OF Connecting Channel
     += ',1PE11.4,' Ft.'/' SLOPE OF THE Connecting Channel = ',1PE11.4)
C
      READ(9,*)B,THET
      WRITE(*,29)B,THET
      WRITE(19,29)B,THET
   29 FORMAT(/' HYDRAULIC EQUIVALENT OF CHANNEL BASE WIDTH = ',1PE11.4,'
     + Ft.'/' ANGLE OF CHANNEL WALL TO THE NORMAL OF THE CHANNEL = ',
     +1PE11.4,' DEG.')
      THET = THET/57.2957795131D0
C
      READ(9,*)XKIA,XKIB
      WRITE(*,30)XKIA,XKIB
      WRITE(19,30)XKIA,XKIB
   30 FORMAT(/' INFILTRATION RATE PER UNIT AREA IN SPREADING AREA A = ',
     +1PE11.4,' Ft./SEC'/' INFILTRATION RATE PER UNIT AREA IN SPREADING
     +AREAS'/' B,C,D, AND OFFSITE = ',1PE11.4,' Ft./SEC')
C
      READ(9,*)XKE
      WRITE(*,31)XKE
      WRITE(19,31)XKE
   31 FORMAT(/' EVAPORATION RATE PER UNIT AREA = ',1PE11.4,' Ft./SEC')
```

```
C
      READ(9,*)XN
      WRITE(*,32)XN
      WRITE(19,32)XN
   32 FORMAT(/' ROUGHNESS COEFFICIENT OF CHANNEL = ',1PE11.4)
C
      READ(9,*)DT
      WRITE(*,33)DT
      WRITE(19,33)DT
   33 FORMAT(/' TIME STEP LENGTH = ',1PE11.4,' SEC')
C
      READ(9,*)ST
      WRITE(*,34)ST
      WRITE(19,34)ST
   34 FORMAT(' START TIME = ',1PE11.4,' SEC')
C
      READ(9,*)ET
      WRITE(*,35)ET
      WRITE(19,35)ET
   35 FORMAT(' STOP TIME = ',1PE11.4,' SEC')
C
      READ(9,*)NPRNT
      WRITE(*,355)
      WRITE(19,355)
  355 FORMAT(' NUMBER OF TIME STEPS BETWEEN PRINT INTERVALS = ',I8)
C
      OPEN(UNIT=10,FILE='A.DAT',STATUS='OLD')
      OPEN(UNIT=11,FILE='BCD.DAT',STATUS='OLD')
      OPEN(UNIT=12,FILE='OFFSIT.DAT',STATUS='OLD')
      REWIND 10
      REWIND 11
      REWIND 12
      WRITE(*,36)
      WRITE(19,36)
   36 FORMAT(/' TABLE OF AREA AND VOLUME VALUES Vs. YA FOR AREA A'/
     +T8,'YA',T24,'AREA',T38,'VOLUME')
      DO 99 I=1,NMAX
      NATB = I
      READ(10,*,END=999)ATAB(I,1),ATAB(I,2),ATAB(I,3)
      WRITE(*,39)ATAB(I,1),ATAB(I,2),ATAB(I,3)
      WRITE(19,39)ATAB(I,1),ATAB(I,2),ATAB(I,3)
   99 CONTINUE
  999 WRITE(*,37)
      WRITE(19,37)
   37 FORMAT(/' TABLE OF AREA AND VOLUME VALUES Vs. YB FOR AREAS BCD'/
     +T8,'YB',T24,'AREA',T38,'VOLUME')
      DO 98 I=1,NMAX
      NBCDTB = I
      READ(11,*,END=998)BCDTAB(I,1),BCDTAB(I,2),BCDTAB(I,3)
      WRITE(*,39)BCDTAB(I,1),BCDTAB(I,2),BCDTAB(I,3)
      WRITE(19,39)BCDTAB(I,1),BCDTAB(I,2),BCDTAB(I,3)
   98 CONTINUE
  998 WRITE(*,38)
      WRITE(19,38)
   38 FORMAT(/' TABLE OF AREA AND VOLUME VALUES Vs. YB FOR OFFSITE AREA'
     +/T8,'YB',T24,'AREA',T38,'VOLUME')
      DO 97 I=1,NMAX
      NOSTB = I
      READ(12,*,END=997)OSTAB(I,1),OSTAB(I,2),OSTAB(I,3)
      WRITE(*,39)OSTAB(I,1),OSTAB(I,2),OSTAB(I,3)
      WRITE(19,39)OSTAB(I,1),OSTAB(I,2),OSTAB(I,3)
   97 CONTINUE
   39 FORMAT(T7,F6.1,T20,1PE11.4,T36,1PE11.4)
C
  997 IF(ISSFLG.EQ.0)THEN
      READ(9,*)CFLOW
      WRITE(*,40)CFLOW
      WRITE(19,40)CFLOW
   40 FORMAT(//' CONSTANT VOLUMETRIC INFLOW FROM DIVERSION CHANNEL =
     +',1PE11.4,' CuFt./SEC')
      ENDIF
      IF(ISSFLG.EQ.1)THEN
      OPEN(UNIT=13,FILE='VFLOW.DAT',STATUS='OLD')
      REWIND 13
      WRITE(*,41)
      WRITE(19,41)
   41 FORMAT(/' TABLE OF VOLUMETRIC INFLOW FOR THE DIVERSION CHANNEL Vs.
```

```
     +TIME'/T8,'TIME',T24,'FLOW RATE')
      DO 96 I=1,NMAX
      NVFTB = I
      READ(13,*,END=996)VFTAB(I,1),VFTAB(I,2)
C CONVERT FROM DAYS TO SECONDS
      WRITE(*,44)VFTAB(I,1),VFTAB(I,2)
      WRITE(19,44)VFTAB(I,1),VFTAB(I,2)
      VFTAB(I,1) = VFTAB(I,1)*86400.D0
   96 CONTINUE
      ENDIF
C
  996 IF(IRAIN.EQ.0)THEN
      READ(9,*)CRAIN
      WRITE(*,42)CRAIN
      WRITE(19,42)CRAIN
   42 FORMAT(/' CONSTANT VOLUMETRIC PRECIPITATION INFLOW PER UNIT AREA =
     +',1PE11.4)
      ENDIF
      IF(IRAIN.EQ.1)THEN
      OPEN(UNIT=14,FILE='RNFLOW.DAT',STATUS='OLD')
      REWIND 14
      WRITE(*,43)
      WRITE(19,43)
   43 FORMAT(/' TABLE OF VOLUMETRIC PRECIPITATION INFLOW PER UNIT AREA
     +Vs. TIME'/T8,'TIME',T24,'FLOW RATE')
      DO 95 I=1,NMAX
      NRNTB = I
      READ(14,*,END=995)RNTAB(I,1),RNTAB(I,2)
      WRITE(*,44)RNTAB(I,1),RNTAB(I,2)
      WRITE(19,44)RNTAB(I,1),RNTAB(I,2)
   95 CONTINUE
      ENDIF
   44 FORMAT(T7,F6.1,T20,1PE11.4)
C
  995 RETURN
      END
C
C
      SUBROUTINE DRAIN(NMAX,ZA,ZB,S,B,THET,XKIA,XKIB,XKE,XN,DT,NPRNT,ST,
     +ET,ATAB,BCDTAB,OSTAB,CFLOW,CRAIN,VFTAB,RNTAB)
C THIS SUBROUTINE .
C
C NRNTB => NUMBER OF DATA POINTS IN RNTAB
      IMPLICIT REAL*8(A-H,O-Z)
      COMMON/FLAGS/ISSFLG,IRAIN,IFLOW
      COMMON/NTABS/NATB,NBCDTB,NOSTB,NVFTB,NRNTB
      DIMENSION ATAB(NMAX,3),BCDTAB(NMAX,3),OSTAB(NMAX,3)
      DIMENSION VFTAB(NMAX,2),RNTAB(NMAX,2)
C
      CALL HEADR
C DETERMINE NUMBER OF TIME STEPS
      NT = (ET-ST)/DT+1.D-6
C INCREMENTAL CHANGE IN ELEVATION FOR SEARCH
      DY = .01D0
C SET PARAMETERS FOR TIME EQUAL ZERO
      VFAI = 0.D0
      OAI = 0.D0
      QAB = 0.D0
      SAI = 0.D0
      VFBI = 0.D0
      OBI = 0.D0
      SBI = 0.D0
      VFOI = 0.D0
      OOI = 0.D0
      SOI = 0.D0
      YBOLD = 0.D0
      YOOLD = 0.D0
C
      DO 99 I=1,NT
      TI1 = I*DT
C 5034 FT. IS BOTTOM OF SPREADING AREA A
      YSA = 5033.D0
C SPREADING AREA A
      ICON = 1
      DO 98 J=2,10000
      YA = YSA+DY*J
      CALL TABLE3(NMAX,NATB,YA,ATAB,AA,SAI1P)
```

```
C DETERMINE INFLOW TO SPREADING AREA A
      IF(ISSFLG.EQ.0)VFAI1=CFLOW
      IF(ISSFLG.EQ.1)CALL TABLE2(NMAX,NVFTB,TI1,VFTAB,VFAI1)
      IF(IRAIN.EQ.0)VFAI1 = VFAI1+CRAIN*AA
      IF(IRAIN.EQ.1)THEN
      CALL TABLE2(NMAX,NRNTB,TI1,RNTAB,RAIN)
      VFAI1 = VFAI1+RAIN*AA
      ENDIF
C DETERMINE OUTFLOW OF SPREADING AREA A
      IF(YA.GT.ZA.AND.YB.LT.ZA)CALL CHANNEL(YA,ZA,B,THET,S,XN,QAB)
C IF CHANNEL IS SUBMERGED
      IF(YA.GT.ZA.AND.YB.GE.ZA)CALL SUBCHAN(YA,YB,ZA,S,B,XN,THET,QAB)
      OAI1 = AA*(XKIA+XKE)+QAB
C DETERMINE IF CONTINUITY OF MASS IS CONSERVED
      CALL MASS(VFAI,VFAI1,OAI,OAI1,SAI,DT,SAI1C)
C AT THE POINT THE INTERPOLATED VOLUME EQUALS COMPUTED VOLUME,
C MASS IS CONSERVED
      CALL TABLE3(NMAX,NATB,YA-1.5D0*DY,ATAB,AA,SLOW)
      CALL TABLE3(NMAX,NATB,YA+1.5D0*DY,ATAB,AA,SHI)
      IF(SAI1C.GE.SLOW.AND.SAI1C.LE.SHI)ICON=0
      IF(ICON.EQ.0)GOTO 97
   98 CONTINUE
C
C SPREADING AREA B
C 5016 FT. IS BOTTOM OF SPREADING AREA B
   97 IF(SBI.EQ.0.D0.AND.QAB.EQ.0.D0)GO TO 95
      YSB = 5015.5D0
      ICON = 1
      DO 96 J=2,10000
      YB = YSB+DY*J
      IF(YB+DY.GE.5053.D0)THEN
      WRITE(*,89)TI1
   89 FORMAT(' DIKE 2 OVERFLOW AT TIME = ',F6.1,'HRS')
      STOP
      ENDIF
      CALL TABLE3(NMAX,NBCDTB,YB,BCDTAB,AB,SBI1P)
C DETERMINE INFLOW TO SPREADING AREA B
      VFBI1 = QAB
      IF(IRAIN.EQ.0)VFBI1 = VFBI1+CRAIN*AB
      IF(IRAIN.EQ.1)THEN
      CALL TABLE2(NMAX,NRNTB,TI1,RNTAB,RAIN)
      VFBI1 = VFBI1+RAIN*AB
      ENDIF
C DETERMINE OUTFLOW OF SPREADING AREA B
      QW = 0.D0
      QBW = 0.D0
      QRW = 0.D0
      IF(YB.GT.5040.AND.YB.LE.5042..AND.YO.LE.5040.)CALL RWEIR(YB,QW)
C IF YB > 5042, THEN DIKE 3 IS OVERTOPPED AND SIMULATES 3250 FT BROAD
C CRESTED WEIR UNTIL YO > 5042
      IF(YB.GT.5042.D0.AND.YO.LE.5040.D0)THEN
      CALL RWEIR(5042.D0,QRW)
      CALL BCWEIR(YB,QBW)
      QW = QRW+QBW
      ENDIF
C
      IF(YB.GT.5040.D0.AND.YB.LE.5042.D0.AND.YO.GT.5040.D0.
     +AND.YO.LE.5042.D0)THEN
      DH = DABS(YB-YO)
      CALL RWEIR(5040.D0+DH,QW)
      ENDIF
C
      IF(YB.GT.5042.D0.AND.YO.LT.5042.D0.AND.YO.GT.5040.D0)THEN
      DH = YO-5040.D0
      CALL RWEIR(5042.D0-.335D0*DH,QRW)
      CALL BCWEIR(YB,QBW)
      QW = QRW+QBW
      ENDIF
C WHEN YO > 5042 THEN THE OFFSITE SPREADING AREA AND SPREADING AREAS
C B, C, AND D SIMULATE ONE LARGE RESERVOIR
      IF(YO.GE.5042.D0.AND.YB.GT.5042.D0)THEN
      YO = YB
      CALL TABLE3(NMAX,NOSTB,YO,OSTAB,AO,SOI1P)
      AB = AB+AO
      ENDIF
      OBI1 = AB*(XKIB+XKE)+QW
C DETERMINE IF CONTINUITY OF MASS IS CONSERVED
```

```
      CALL MASS(VFBI,VFBI1,OBI,OBI1,SBI,DT,SBI1C)
C AT THE POINT THE INTERPOLATED VOLUME EQUALS COMPUTED VOLUME,
C MASS IS CONSERVED
      CALL TABLE3(NMAX,NBCDTB,YB-1.5D0*DY,BCDTAB,AX,SLOW)
      CALL TABLE3(NMAX,NBCDTB,YB+1.5D0*DY,BCDTAB,AX,SHI)
      IF(SBI1C.GE.SLOW.AND.SBI1C.LE.SHI)ICON=0
      IF(ICON.EQ.0.AND.YO.EQ.0.D0.AND.DABS(YBOLD-YB).LT.0.005D0.
     &AND.ISSFLG.EQ.0)THEN
      CALL OUTPUT(TI1,YA,YB,YO,SAI,SBI,SOI,QAB,QW,QBW)
      WRITE(19,101)TI1/3600.D0
      WRITE(*,101)TI1/3600.D0
  101 FORMAT(/' STEADY-STATE AT TIME = ',F6.1,' HRS')
      STOP
      ENDIF
      IF(ICON.EQ.0)GOTO 95
   96 CONTINUE
C
C OFFSITE SPREADING AREA
C 5020 FT. IS BOTTOM OF OFFSITE SPREADING AREA
   95 IF(SOI.EQ.0.D0.AND.QW.EQ.0.D0)GO TO 93
      IF(YO.GE.5042.D0.AND.YB.GT.5042.D0)GO TO 93
      YSO = 5019.D0
      ICON = 1
      DO 94 J=2,10000
      YO = YSO+DY*J
      CALL TABLE3(NMAX,NOSTB,YO,OSTAB,AO,SOI1P)
C DETERMINE INFLOW TO SPREADING AREA A
      VFOI1 = QW
      IF(IRAIN.EQ.0)VFOI1 = VFOI1+CRAIN*AO
      IF(IRAIN.EQ.1)THEN
      CALL TABLE2(NMAX,NRNTB,TI1,RNTAB,RAIN)
      VFOI1 = VFOI1+RAIN*AO
      ENDIF
C DETERMINE OUTFLOW OF OFFSITE SPREADING AREA
      OOI1 = AO*(XKIB+XKE)
C DETERMINE IF CONTINUITY OF MASS IS CONSERVED
      CALL MASS(VFOI,VFOI1,OOI,OOI1,SOI,DT,SOI1C)
C AT THE POINT THE INTERPOLATED VOLUME EQUALS COMPUTED VOLUME,
C MASS IS CONSERVED
      CALL TABLE3(NMAX,NOSTB,YO-1.5D0*DY,OSTAB,AX,SLOW)
      CALL TABLE3(NMAX,NOSTB,YO+1.5D0*DY,OSTAB,AX,SHI)
      IF(SOI1C.GE.SLOW.AND.SOI1C.LE.SHI)ICON=0
      IF(ICON.EQ.0.AND.DABS(YBOLD-YB).LT.5.D-03.AND.DABS(YOOLD-YO).
     +LT.5.D-03.AND.ISSFLG.EQ.0)THEN
      CALL OUTPUT(TI1,YA,YB,YO,SAI,SBI,SOI,QAB,QW,QBW)
      WRITE(19,102)TI1/3600.D0
      WRITE(*,102)TI1/3600.D0
  102 FORMAT(/' STEADY-STATE AT TIME = ',F6.1,' HRS')
      STOP
      ENDIF
      IF(ICON.EQ.0)GOTO 93
   94 CONTINUE
C
C UPDATE FOR NEXT TIME STEP
   93 VFAI = VFAI1
      OAI = OAI1
      SAI = SAI1C
      VFBI = VFBI1
      OBI = OBI1
      SBI = SBI1C
      VFOI = VFOI1
      OOI = OOI1
      SOI = SOI1C
      YBOLD = YB
      YOOLD = YO
      CALL OUTPUT(TI1,YA,YB,YO,SAI,SBI,SOI,QAB,QW,QBW)
   99 CONTINUE
      RETURN
      END
C
      SUBROUTINE HEADR
      IMPLICIT REAL*8(A-H,O-Z)
      WRITE(*,99)
      WRITE(19,99)
   99 FORMAT('1',T2,'TIME',T8,'A WTR ELEV.',T21,'BCD WTR ELEV.',T36,
     +'OFFSITE ELEV.',T51,'A VOLUME',T62,'BCD VOLUME',T74,'OFFSITE VOL.'
     +,T88,'CONN. CHNL. FLOW',T107,'WEIR FLOW',T119,'DIKE 3 OVRFLOW')
```

```
      WRITE(*,98)
      WRITE(19,98)
   98 FORMAT(T2,'(HRS)',T10,'(FEET)',T24,'(FEET)',T39,'(FEET)',T51,
     +'(Cu.Ft.)',T63,'(Cu.Ft.)',T76,'(Cu.Ft.)',T90,'(Cu.Ft./SEC)',T105,
     +'(Cu.Ft./SEC)',T120,'(Cu.Ft./SEC)')
      RETURN
      END
C
      SUBROUTINE OUTPUT(TI1,YA,YB,YO,SA,SB,SO,QAB,QW,QBW)
      IMPLICIT REAL*8(A-H,O-Z)
      QRW = DABS(QW-QBW)
      WRITE(*,99)TI1/3600.D0,YA,YB,YO,SA,SB,SO,QAB,QRW,QBW
      WRITE(19,99)TI1/3600.D0,YA,YB,YO,SA,SB,SO,QAB,QRW,QBW
   99 FORMAT(T2,F6.1,T10,F7.2,T24,F7.2,T39,F7.2,T49,E11.4,T61,E11.4,
     +T74,E11.4,T90,F8.2,T105,F8.2,T120,F8.2)
      RETURN
      END
C
      SUBROUTINE RWEIR(Y,Q)
C CALCULATES THE VOLUMETRIC FLOW OUT OF THE RECTANGULAR WEIR AT DIKE 3.
C FLOW BEGINS AT 5040 FT. MSL.
C Y => ELEVATION
C
      IMPLICIT REAL*8(A-H,O-Z)
      Q = 284.84D0*((Y-5040.D0)**1.5D0)
      RETURN
      END
C
      SUBROUTINE BCWEIR(Y,Q)
C CALCULATES THE VOLUMETRIC FLOW OVER DIKE 3 BY SIMULATING A 3250 FT
C BROAD CRESTED WEIR FLOW BEGINS AT 5042 FT. MSL.
C Y => ELEVATION
C
      IMPLICIT REAL*8(A-H,O-Z)
      Q = (1.0033D+04)*((Y-5042.D0)**1.5D0)
      RETURN
      END
C
      SUBROUTINE SUBCHAN(YA,YB,ZA,S,B,XN,THET,Q)
C THIS SUBROUTINE USES A SIMPLIFIED FORM OF THE ST. VENNANT EQS.
C TO SOLVE FOR THE FLOW RATE IN THE Connecting Channel WHEN THE
C FLOW IS SUBMERGED.
      IMPLICIT REAL*8(A-H,O-Z)
C NORMAL CHANNEL DEPTH
      YN = YA-ZA
C AREA
      A = YN*(B+YN*DTAN(THET))
C WETTED PERIMETER
      P = B+2.D0*YN/DCOS(THET)
C GRAVITATION CONSTANT
      G = 32.2D0
C DO SEARCH TO FIND Q
      DO 99 Q=Q/1.1D0,10000.D0,2.D0
      V = Q/A
      ACC =((V**2)-G*A/B)*(YA-YB)
      POT = -G*(A/B)*(YN/S)*((Q*XN/1.49D0)*(A**(-5.D0/3.D0))*
     &(P**(2.D0/3.D0)))**2
      IF(POT.LE.ACC)GO TO 98
   99 CONTINUE
   98 RETURN
      END
C
      SUBROUTINE CHANNEL(YA,ZA,B,THET,S,XN,QAB)
C THIS SUBROUTINE EMPLOYS THE MANNING EQUATION TO CALCULATE THE
C VOLUMETRIC FLOW IN THE CHANNEL BETWEEN SPREADING AREA A AND B
C YA => WATER SURFACE ELEVATION OF SPREADING AREA A
C ZA => ELEVATION OF INLET TO CONNECTING CHANNEL
C S => SLOPE OF CONNECTING CHANNEL
C B => HYDRAULIC EQUIVALENT OF CHANNEL BASE WIDTH
C THET => ANGLE OF CHANNEL WALL DEPARTURE FROM THE NORMAL TO THE CHANNEL
C XN => ROUGHNESS COEFFICIENT OF CHANNEL
C QAB => VOLUMETRIC FLOW IN THE CHANNEL BETWEEN SPREADING AREA A AND B
C
      IMPLICIT REAL*8(A-H,O-Z)
      QAB = (1.49D0/XN)*((((YA-ZA)*(B+(YA-ZA)*DTAN(THET)))**(1.D0+
     &2.D0/3.D0))*(B+2.D0*(YA-ZA)/DCOS(THET))**(-2.D0/3.D0))*DSQRT(S)
      RETURN
```

```
      END
C
      SUBROUTINE MASS(VFLWI,VFLWI1,OI,OI1,SI,DT,SI1)
C THIS SUBROUTINE CALCULATES THE DIFFERENCE BETWEEN VOLUMETRIC INFLOW
C AND OUTFLOW USING THE CONTINUITY OF MASS EQUATION ADAPTED FOR
C RESERVOIRS
C VFLWI => VOLUMETRIC INFLOW INTO THE RESERVOIR AT TIME I
C VFLWI1 => VOLUMETRIC INFLOW INTO THE RESERVOIR AT TIME I+1
C OI => VOLUMETRIC OUTFLOW OUT OF THE RESERVOIR AT TIME I
C OI1 => VOLUMETRIC OUTFLOW OUT OF THE RESERVOIR AT TIME I+1
C SI => STORAGE (VOLUME) OF RESERVOIR AT TIME I
C SI1 => STORAGE (VOLUME) OF RESERVOIR AT TIME I+1
C DT => TIME STEP LENGTH
C DMASS => DIFFERENCE BETWEEN VOLUMETRIC INFLOW AND (OUTFLOW PLUS
C STORAGE RATE) OF RESERVOIR
C
      IMPLICIT REAL*8(A-H,O-Z)
      SI1 = ((VFLWI+VFLWI1)/2.D0-(OI+OI1)/2.D0)*DT+SI
      RETURN
      END
C
      SUBROUTINE TABLE3(NMAX,NOP,Y,TAB,A,V)
C THIS SUBROUTINE USES LINEAR INTERPOLATION FOR A AND V Vs. Y
C NOP => NUMBER OF POINTS IN THE TABLE
C TAB => TABLE
C Y => ELEVATION
C A => AREA
C V => VOLUME
C
      IMPLICIT REAL*8(A-H,O-Z)
      DIMENSION TAB(NMAX,3)
      LOC = 0
      DO 99 I=1,NOP-1
      IF(Y.GE.TAB(I,1).AND.Y.LT.TAB(I+1,1))THEN
      LOC = I
      GOTO 98
      ENDIF
   99 CONTINUE
   98 IF(LOC.EQ.0.OR.LOC.EQ.NOP)THEN
      WRITE(*,*)' *********TABLE CANNOT DO EXTRAPOLATION 3 ******'
      STOP
      ENDIF
      A = -(TAB(LOC,2)-TAB(LOC+1,2))*(TAB(LOC,1)-Y)/(TAB(LOC,1)-
     &TAB(LOC+1,1))+TAB(LOC,2)
      V = -(TAB(LOC,3)-TAB(LOC+1,3))*(TAB(LOC,1)-Y)/(TAB(LOC,1)-
     &TAB(LOC+1,1))+TAB(LOC,3)
      RETURN
      END
C
      SUBROUTINE TABLE2(NMAX,NOP,T,TAB,F)
C THIS SUBROUTINE USES LINEAR INTERPOLATION FOR F Vs. Y
C NOP => NUMBER OF POINTS IN THE TABLE
C TAB => TABLE
C T => TIME
C F => VOLUMETRIC FLOW RATE
C
      IMPLICIT REAL*8(A-H,O-Z)
      DIMENSION TAB(NMAX,2)
C
      LOC = 0
      DO 99 I=1,NOP-1
      IF(T.GE.TAB(I,1).AND.T.LT.TAB(I+1,1))THEN
      LOC = I
      GOTO 98
      ENDIF
   99 CONTINUE
   98 IF(LOC.EQ.0.OR.LOC.EQ.NOP)THEN
      WRITE(*,*)' *********TABLE CANNOT DO EXTRAPOLATION 2 ******'
      STOP
      ENDIF
      F = -(TAB(LOC,2)-TAB(LOC+1,2))*(TAB(LOC,1)-T)/(TAB(LOC,1)-
     &TAB(LOC+1,1))+TAB(LOC,2)
      RETURN
      END
```